ROLE OF CHOLESTEROL SULFOTANSFERASE AND STEROID SULFATASE IN NUCLEAR RECEPTOR MEDIATED ENERGY HOMEOSTASIS

by

Yuhan Bi

Bachelor of Science, Georgia State University, 2013

Submitted to the Graduate Faculty of

School of Pharmacy in partial fulfillment

of the requirements for the degree of

Doctor of Philosophy

University of Pittsburgh

2018

UNIVERSITY OF PITTSBURGH

SCHOOL OF PHARMACY

This dissertation was presented

by

Yuhan Bi

It was defended on

March 13th 2018

and approved by

Kyle W. Selcer, Associate Professor, Biological Sciences

Lisa C. Rohan, Professor, Pharmaceutical Sciences

Xiaochao Ma, Associate Professor, Pharmaceutical Sciences

Da Yang, Assistant Professor, Pharmaceutical Sciences

Dissertation Advisor: Wen Xie, Professor, Pharmaceutical Sciences

ROLE OF CHOLESTEROL SULFOTANSFERASE AND STEROID SULFATASE IN NUCLEAR RECEPTOR MEDIATED ENERGY HOMEOSTASIS

Yuhan Bi

University of Pittsburgh, 2018

The cholesterol sulfotransferase SULT2B1b converts cholesterol to cholesterol sulfate (CS). We previously reported that SULT2B1b inhibits hepatic gluconeogenesis by antagonizing the gluconeogenic activity of hepatocyte nuclear factor 4 (HNF4α). In this study, we showed that the SULT2B1b gene is a transcriptional target of HNF4α, which led to our hypothesis that the induction of SULT2B1b by HNF4 represents a negative feedback to limit the gluconeogenic activity of HNF4α. Indeed, downregulation of Sult2B1b enhanced the gluconeogenic activity of HNF4α, which may have been accounted for by the increased acetylation of HNF4 as a result of decreased expression of the HNF4 deacetylase sirtuin 1 (Sirt1). The expression of Sult2B1b was also induced by HNF4 upon fasting, and the Sult2B1b null (Sult2B1b$^{-/-}$) mice showed increased gluconeogenic gene expression and an elevated fasting glucose level, suggesting that SULT2B1b also plays a restrictive role in HNF4 -mediated fasting-responsive gluconeogenesis. We also developed thiocholesterol, a hydrolysis-resistant derivative of CS, which showed superior activity to that of the native CS in inhibiting gluconeogenesis and improving insulin sensitivity in high-fat-diet-induced diabetic mice. We conclude that the HNF4 -SULT2B1b-CS axis represents a key

endogenous mechanism to prevent uncontrolled gluconeogenesis. Thiocholesterol may be used as a therapeutic agent to manage hyperglycemia.

Steroid sulfatase (STS), a desulfating enzyme that converts steroid sulfates to hormonally active steroids, plays an important role in the homeostasis of sex hormones. STS is expressed in the adipose tissue of both male and female mice, but the role of STS in the development and function of adipose tissue remains largely unknown. In this report, we first showed that the adipose expression of Sts was induced in the high-fat diet (HFD) and ob/ob models of obesity and type 2 diabetes. Transgenic overexpression of the human STS in the adipose tissue of male mice exacerbated the HFD induced metabolic phenotypes, including increased body weight gain and fat mass, and worsened insulin sensitivity, glucose tolerance and energy expenditure, which were accounted for by adipocyte hypertrophy, increased adipose inflammation, and dysregulation of adipogenesis. The metabolic harm of the STS transgene appeared to have resulted from increased androgen activity in the adipose tissue, and castration abolished most of the phenotypes. Interestingly, the transgenic effects were sex-specific, because the HFD-fed female STS transgenic mice exhibited improved metabolic functions, which were associated with attenuated adipose inflammation. The metabolic benefit of the STS transgene in female mice was accounted for by increased estrogenic activity in the adipose tissue, whereas such benefit was abolished upon ovariectomy. Our results revealed an essential role of the adipose STS in energy homeostasis in sex- and sex hormone-dependent manner. The adipose STS may represent a novel therapeutic target for the management of obesity and type 2 diabetes.

In summary, I have uncovered novel roles and mechanisms of SULT2B1b and STS in HNF4α mediated hepatic gluconeonenesis and in estrogen receptor (ER)/ androgen receptor (AR) mediated energy homeostasis of adipose tissue respectively, which may facilitate the development of novel interventions for metabolic syndromes.

TABLE OF CONTENTS

LIST OF PICTURES

LIST OF FIGURES

PREFACE

This thesis is dedicated to my parents, without them I would have no passion and courage to pursue my goal in life; to my boss Dr. Wen Xie, who offers me generous guidance and patience to let me grow as a scientist; and to my dear friends and colleagues, who share my happiness and sorrow.

ABBREVIATION

ACC, acetyl-CoA carboxylase; **AR**, androgen receptor; **BAT**, brown adipose tissue; **CAR,** constitutive androstane receptor; **ChIP**, chromatin immunoprecipitation; **CS**, cholesterol sulfate; **DHEA**, dehydroepiandrosterone; **DMSO**, Dimethyl sulfoxide; **DOX**, doxycycline; **EMSA**, Electrophoretic mobility shift assay; **ER**, estrogen receptor; **EST**, estrogen sulfotransferases; **FABP**, fatty acid binding protein; **FAS**, fatty acid synthase; **FAT/CD36**, fatty acid translocase; **FABP**, fatty acid binding protein; **FBS**, fetal bovine serum; **FFA**, free fatty acid; **FoxA2**, forkhead factor A2; **FoxO1**, forkhead transcription factor O1; **FSK,** forskolin; **FXR,** farnesoid X receptor; **G6pase**, glucose-6-phosphatase; **GLUT4**, glucose transporter 4; **HFD**, high-fat diet; **H&E**, Haematoxylin Eosin; **HFD,** high-fat diet; **HNF4α**, hepatocyte nuclear factor 4α;**IHC**, immunohistochemistry; **IL-1**, interleukin-1; **IL-6**, interleukin-6; **IPGTT**, intraperitoneal glucose tolerance test; **IRS**, insulin receptor substrate; **ITT**, insulin tolerance test; **LPL**, lipoprotein lipase; **LXR**, liver X receptor; **MAPK**, mitogen-activated protein kinases; **MCP-1**, monocyte chemoattractant protein-1; **PAPS**, 3- phosphoadenosine-5-phosposulfate; **PCR,** Polymerase chain reaction**; PEPCK**, phosphoenolpyruvate carboxykinase; **PGC-1a**, PPARg coactivator-1a; **PEPCK**, phosphoenolpyruvate carboxykinase; **PPAR α**, peroxisome proliferator-activated receptor α; **PPAR γ**, peroxisome proliferator-activated receptor γ; **PXR**, pregnane X receptor; **RXR**, retinoid X receptor; **SREBP**, Sterol Regulatory Element-Binding Proteins; **STS**, steroid sulfatase; **SULT,** sulfotransferase**; T2D,** type 2 diabetes;**SREBP-1c**, sterolxiiregulatory element-binding protein 1c; **STS**, steroid sulfatase; **SULT2B1b**, cholesterol sulfotransferases; **SULTs**,

sulfotransferases (SULTs); **TCPOBOP**, 1,4-Bis-[2-(3,5-dichloropyridyloxy)]benzene, 3,3′,5,5′-Tetrachloro-1,4-bis(pyridyloxy)benzene; **TH**, thiocholesterol; **TG**, transgenic; **TNFα**, tumor necrosis factor α; **TRE**, tetracycline response element; **tTA**, tetracycline transactivator; **VMN**, ventromedial hypothalamic nucleus; **WAT**, white adipose tissue; **WT**, wild type; **XBP1**, X-box binding protein 1.

1.0 **CHAPTER I: NUCLEAR RECEPTORS AND METABOLIC REGULATIONS**

Nuclear receptors are a group of ligands binding transcriptional factors. Through regulating the expression of target genes, they could regulate physiological processes including reproduction, development, and energy metabolism. In the early-1980s, the early several members of steroid receptors are first recognized as the sensors and mediators of steroid hormone signaling. The subsequent cloning of other nuclear receptor genes based on sequence similarity unexpected revealed a large family of nuclear receptor-like genes. There is a total of 48 members discovered of transcriptional factor family including the classic endocrine receptors and many so-called orphan receptors whose ligands (1 and 2).

Classic nuclear steroid hormone receptors included the glucocorticoid (GR), mineralocorticoid (MR), estrogen (ER), androgen (AR), and progesterone (PR) receptors. Steroid hormones are synthesized mainly from endogenous endocrine sources that are regulated by negative-feedback control of the hypothalamic-pituitary axis. Steroid hormones are circulated in the body to their target tissues where they bind to their receptors with high affinity (within nM range). Upon hormone binding, steroid receptors bind to DNA as homodimers, and regulate its target genes expression. Steroid receptors are well documented to regulate a variety of metabolic

and developmental process including sexual differentiation, reproduction, energy metabolism, and electrolyte balance (3).

Orphan nuclear receptors include receptors for fatty acids (peroxisome proliferator-activated receptors; PPARs), oxysterols (Liver X receptors; LXRs), bile acids (farnesoid X receptor; FXR), xenobiotics (pregnane X receptor; PXR and constitutive androstane receptor; CAR). The hepatic nuclear receptor (HNF4α) is also one member of the orphan nuclear receptor family. Generally, these receptors bind their hydrophobic lipid ligands with relatively lower affinities within μM range. During the past decades, researchers have uncovered the significant physiological roles, including reproductive biology, inflammation, cancer, diabetes, cardiovascular disease, and obesity. These receptors functions as sensors to maintain energy homeostasis through regulating the transcription of a family of genes involved in energy metabolism, storage, transport, and elimination (4).

.

My thesis projects mainly focus on the mediated roles of three of these nuclear receptors (the orphan nuclear receptor HNF4α, and nuclear steroid hormone receptors ER and AR) in energy homeostasis and metabolic syndromes.

1.1 ROLE OF HNF4α IN GLUCOSE METABOLISM

The hepatocyte nuclear factor 4 (HNF4α) is a liver-enriched orphan nuclear receptor that plays a pivotal role in energy homeostasis by regulating the metabolism of glucose and lipids (5, 6). HNF4α promotes gluconeogenesis through its positive regulation of PEPCK and G6Pase genes (7, 8). Although the HNF4α-promoted gluconeogenesis is physiologically essential, uncontrolled gluconeogenesis is a major pathogenic event in the development of T2D (9–11). The expression and activity of HNF4 are elevated in response to fasting, which is essential to maintain the fasting glucose level (9). Increased gluconeogenesis is also responsible for the increased whole-body glucose production in T2D patients after an overnight fasting (10, 11). The activity of HNF4 can be regulated by posttranslational modifications, including acetylation (12). The acetylation homeostasis of HNF4 is controlled by both deacetylases, such as sirtuin 1 (Sirt1) (13), and acetylates, such as CBP/p300 (14).

1.2 ROLE OF ENDOCRINE NUCLEAR RECEPTORS ER AND AR IN ENERGY HOMEOSTASIS

In addition to reproduction, sex hormones, including estrogens and androgens, are implicated in various physiological functions, including energy homeostasis (15 and 16). Postmenopausal women have increased risk of developing metabolic syndromes, such as obesity and insulin resistance type 2 diabetes. Estrogen replacement therapies ameliorate metabolic disorders and decreased abdominal fat gain in women and rodent models (17 and 18). Human subjects lacking Estrogen receptor α (ERα) or aromatase, the primary enzyme converting androgens to estrogens were found to develop insulin resistance and obesity (19-21). Additionally, mice deficient of aromatase were also reported to develop obesity due to reduced physical activity and decreased lean body mass (22 and 23). The deficiencies of estrogens also lead to impaired insulin sensitivity and adiposity in both aromatase knockout (21) and Erα deficient (22) mice. On the other hand, estrogens administration improves insulin sensitivity and adiposity in HFD fed female mice (24) and in ob/ob mice (25). In general, estrogen plays a beneficial role to improve energy homeostasis in both male and female. The effects of estrogen on fat have been reported, while most are accounted on whole body effect of estrogen or certain peripheral tissues like liver and brain. The adipose tissue (AT) specific role of estrogen in energy homeostasis is still unclear.

The role of androgen in energy homeostasis has also been studied (26). Unlike estrogen, the role of androgen shows sexual dimorphisms. In female, excess androgenic activity in liver, skeletal muscle, pancreatic β-cells, and metabolic centers in the hypothalamus synergize to worsen metabolic function, inflammation, visceral adiposity, and T2D (26-33). While, in male low testosterone predisposes to diabetes and hyperglycemia and low-level testosterone is associated

with diabetes (34-36). The tissue specific roles of androgen in central system and several peripheral tissues including liver, pancreatic β-cells, and skeletal muscle in male have been established. Androgen through activating AR could inhibit hepatic lipogenesis, promote hepatic lipid oxidation, improve insulin sensitivity and prevent hepatic steatosis (37- 39). Androgen also improved pancreatic β-cell function and increase insulin secretion, which could be important implications for prevention of T2D in hypoandrogenic men (40 and 41). Testosterone deficiency promotes insulin resistance in skeletal muscle at least partially via an AR- dependent mechanism involving a decrease in PGC1a-mediated oxidative and insulin sensitive muscle fibers (42). Although, it is known that testosterone deficiency leads to visceral obesity in men and there is an inverse correlation between total serum testosterone and the amount of visceral adipose tissue (43 and 44). This has been reported to be indirectly mediated via AR actions in muscle (45-48). The direct effect of androgen on adiposity and AT energy homeostasis is unclear.

2.0 CHOLESTEROL SULFOTRANSFERASE (SULT2B1B) AND STEROID SULFATASE (STS) IN ENERGY METABOLISM

As mentioned, the nuclear receptors function as sensors to maintain energy homeostasis through regulating the transcription of a family of genes involved in energy metabolism, storage, transport, and elimination. The biological functions of these "sensors" are highly related to the nutrients themselves, and therefore the cross talk between nutrients and nutrient sensors form feed-back regulations to maintain physical homeostasis. On the other hand, there are classes of metabolizing enzymes responsible for the chemical and biological balance of the nutrients, which including the Cholesterol Sulfotransferase (SULT2B1b) and the Steroid Sufatase (STS). In my thesis study, I dedicated to investigating of the roles of these two nutrients metabolism enzymes in energy homeostasis through the mediation of nuclear receptors.

2.1 CHOLESTEROL SULFOTRANSFERASE (SULT2B1B) AND ITS ENZYMATIC PRODUCTS CHOLESTEROL SULFATE (CS)

Sulfotransferases (SULTs) catalyze the transfer of a sulfate group from 3-phosphoadenosine 5-phosphosulfate (PAPS) to an acceptor molecule (49). Sulfation plays an essential role in regulating the chemical and functional homeostasis of endogenous and exogenous molecules (50 and 51).

The mouse SULT2B1 hydroxysteroid sulfotransferase (designated SULT2B1a) has two isoforms the SULT2B1b gene and the later cloned SULT2B1a gene. These two isoforms are akin with each other, and in fact derived from the same gene as a result of an alternative exon 1 and differential splicing. Thus, the two isoforms differ only at their amino termini. The identical gene structure of mouse SULT2B1 gene and human SULT2B1 gene indicates that this gene and its products are highly conserved within mouse and human. However, the cloned mouse SULT2B1a isoform is lightly different from its human counterpart in its gene structure. In comparison to the unique amino terminus of human SULT2B1a with only 8 amino acids, mouse SULT2B1a is 54 amino acids in length. While the lengths of the unique amino terminus for the mouse and human SULT2B1b isoforms are quite similar, at 20 and 23 amino acids, respectively. The longer amino terminus of mouse SULT2B1a accounts for its being approximately 5% larger than SULT2B1b, which is the opposite of the case with the human counterparts, where SULT2B1b is larger than SULT2B1a. In addition to the structural distinction between human and mouse SULT2B1a, they also differ functionally (52). Mouse SULT2B1a efficiently sulfonates cholesterol with the highest kcat/Km ratios, however human SULT2B1a sulfonates cholesterol very weakly (53).

Differential expression patterns of SULT2B1a and SULT2B1b in organ systems, particularly the skin and brain, in association with their respective substrate preferences reveal potential physiological implications for the sulfonated product. SULT2B1b, now recognized as a cholesterol sulfotransferase, is quantitatively the predominant hydroxysteroid sulfotransferase expressed in human skin. The human fetal brain appears to only express the SULT2B1a isoform which is consistent with the evidence that the brain and spinal cord in mouse almost exclusively express SULT2B1a (54). SULT2B1b is expressed in multiple tissues, including the liver (54-56). Although the mouse liver does not have a high basal expression of SULT2B1b (56), the hepatic expression of SULT2B1b is highly inducible, such as in response to TCPOBOP, an agonist for the constitutive androstane receptor (CAR) (56).

As mentioned, the primary enzymatic byproduct of SULT2B1b, is Cholesterol sulfate, a predominant steroid sulfate in the circulation. Cholesterol sulfate concentrations in human plasma range from 134-254 ug/ml (57 and 58). Cholesterol sulfate is also present in various body fluids and tissues, including urine, bile, seminal plasma, skin, adrenal, kidney and liver (55 and 59). Despite its prevalence and abundance, the physiological role of CS remains to be defined. Cholesterol sulfate has been recognized to be essential in skin development as a regulatory molecule in human keratinocyte differentiation and creation of the barrier (6 and 70). In vitro studies showed CS is a nature agonist for the retinoic acid-related orphan receptor (ROR) (60). It was suggested that CS may play a role in immune response and a shortage of CS in fetus may contribute to the development of autism (61). Cholesterol sulfate is also a major cell surface

substance that is essential for the cell membrane function (62). Previously, Shi published that SULT2B1b and CS could inhibit HNF4α mediated gluconeogenesis (6).

2.2 ROLE OF STEROID SULFOTASE (STS) IN ENERGY HOEMEOSTASIS

Steroid Sulfatase (STS), also known as aryl sulfatase C, is an enzyme responsible for the cleavage of steroid sulfate to active steroid, most important examples are reversing estrone sulfate to estrone and dehydroepiandrosterone sulfate (DHEA-S) to DHEA (63). Pregnenolone sulfate and cholesterol sulfate are the other two important substrates of STS. Steroids are mostly existing in sulfate form, as in the case of DHEA-S, which is present in concentrations up to 100-fold higher than unconjugated DHEA (64). The half-life of steroid sulfate is also relatively long in comparison with active steroids. For instance, estrone sulfate is very abundant in human serum with concentrations 10–20-fold higher than estrone and estradiol (65). The expression of STS is confirmed not only in reproductive organs like the ovaries, placenta, testis, endometrium, but also in the adrenal glands, kidney, bone, skin and fat tissue brain, fetal lung, lymphocytes, aorta (66).

Steroid sulfonation and de-conjugation pathways play an important role in steroid chemical and biological homeostasis. Steroid sulfatase (STS) converts cholesterol sulfate to cholesterol, which is then transported into mitochondria for conversion to pregnenolone, and downstream adrenal products including DHEA and DHEA sulfate. DHEA sulfate serves as the precursor molecule for synthesis of the non-adrenal steroid hormones, including testosterone and estrogens (67-69). Therefore, STS is involved in many physiological and pathophysiological conditions based on the biological roles of its substrates. Inactivation of the STS gene results in X-linked

ichthyosis due to excess deposition of cholesterol sulfate in the skin (70). As mentioned in 1.2, estrogen and androgen dysregulation is always associated with increased risk of obesity, insulin resistance, diabetes, or cardiovascular disease (71). STS is the main sulfates to synthesize the active sex hormones (estrogens and androgens), the role of STS activity in metabolism is more complex and seems to be sex specific. Previously Jiang reported that the beneficial role STS in hepatic energy homeostasis in both genders but via distinct mechanisms. The metabolic benefit in female transgenic mice specifically expressing STS in the liver was likely mediated by increased hepatic estrogen activity, whereas the protective effect of STS in males may have been accounted by decreased inflammation in white adipose tissue (72). STS is also expressed in the white adipose tissue of women where it plays an important role in the formation of biologically active sex hormones, especially in postmenopausal women. Both the expression and activity of STS were higher in postmenopausal adipose tissues than in premenopausal adipose tissues, which might suggest that the hydrolysis of circulating steroid-S may have played an increasing role after menopause in local steroid biosynthesis in the adipose tissue (73).

3.0 CHAPTER III: REGULATION OF CHOLESTEROL SULFOTRANSFERASE SULT2B1B BY HEPATOCYTE NUCLEAR FACTOR 4 A CONSTITUTES A NEGATIVE FEEDBACK CONTROL OF HEPATIC GLUCONEOGENESIS

Hepatic gluconeogenesis and lipogenesis are two critical components of energy metabolism. Previous studies have suggested a critical role of SULT2B1b in hepatic energy homeostasis. SULT2B1b can inhibit lipogenesis by sulfonating and deactivating oxysterols, the endogenous agonists for the lipogenic nuclear receptor liver X receptor (LXR) (51). The expression and regulation of Sult2B1b were found to be important for the antilipogenic activity of CAR (56). We recently reported that SULT2B1b and its enzymatic by-product CS attenuated hepatic gluconeogenesis by inhibiting HNF4α and increased serum leptin level to inhibit obese induced metabolic disorder (6). HNF4α has diverse functions, including its regulation of hepatic gluconeogenesis by positively regulating the gluconeogenic enzymes phosphoenolpyruvate carboxykinase (PEPCK) and glucose 6-phosphatase (G6Pase). Interestingly, we found that the expression of SULT2B1b was positively regulated by HNF4α. In this case, SULT2B1b and HNF4α may form a negative feedback mechanism to regulate HNF4α mediated gluconeogenesis. In this study, our goal is to demonstrate the positive regulation of SULT2B1b by HNF4α and to investigate the physiological meaning of this negative feedback regulation in hepatic gluconeogenesis.

PIC 1

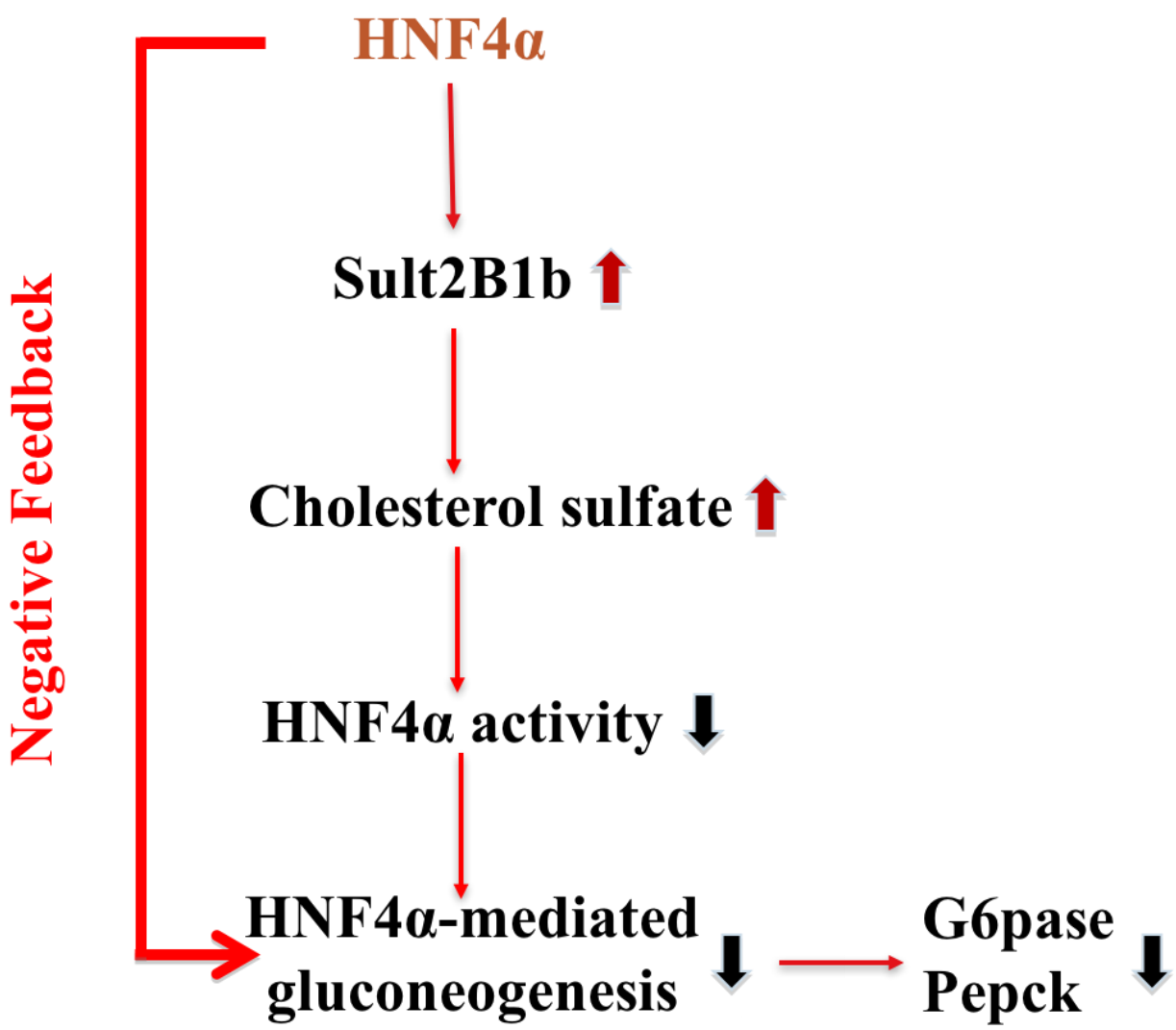

Picture 1. Description of the negative feedback regulation between HNF4α and SULT2B1b.

3.1 METHOD

3.1.1 Mice, diet, and chemicals.

The Sult2B1b$^{-/-}$ mice (strain number 018773) were obtained from the Jackson Laboratory (Bar Harbor, ME). Standard chow from PMI Nutrition (St. Louis, MO) or HFD (S3282) from Bio-serv (Frenchtown, NJ) was used. All chemicals were purchased from Sigma (St. Louis, MO).

3.1.2 Isolation of mouse and human primary hepatocytes.

Mouse primary hepatocytes were isolated by collagenase perfusion from 8-week-old male wild-type or Sult2B1b$^{-/-}$ mice as we have previously described (6). Human primary hepatocytes, also isolated by collagenase perfusion, were obtained through the NIH-sponsored Liver Tissue Procurement and Distribution System at the University of Pittsburgh.

3.1.3 Histological and serum insulin analysis.

For Oil red O staining, snap-frozen liver tissues were sectioned into 8- m-thick samples and stained in 0.5% Oil red O in propylene glycerol. The serum insulin level was measured by an assay kit (catalog number 90080) from Crystal Chem (Downers Grove, IL).

3.1.4 Immunoprecipitation, Western blot analysis, and ChIP assays.

Immunoprecipitation and Western blot analysis were performed as described previously (6). The primary antibody used for HNF4 (catalog number MA1-199) was purchased from

ThermoFisher Scientific (Pittsburgh, PA). Anti-acetylated lysine (catalog number 9441S), anti-Sirt1 (D60E1), and anti-FLAG (catalog number 2368) antibodies were purchased from Cell Signaling (Danvers, MA). The anti-Acss (sc-85258) and anti-SULT2B1b (sc-67103) antibodies were purchased from Santa Cruz (Santa Cruz, CA). Western blotting images were quantified with the ImageJ software (http://rsb.info.nih.gov/ij/). The ChIP assay was performed as we have previously described (6).

3.1.5 Glucose production assay.

Cells were washed three times with phosphate-buffered saline (PBS) to remove glucose. Cells were then incubated in glucose production buffer (glucose-free Dulbecco's modified Eagle medium [DMEM] [pH 7.4] containing 20 mM sodium lactate and 2 mM sodium pyruvate without phenol red) for 4 h, after which 500 l of medium was removed and centrifuged at 15,000 *g* for 10 min. The glucose content in the supernatant was measured with a glucose assay kit from Sigma. Glucose concentrations were normalized to cellular protein concentrations.

3.1.6 Immunofluorescence.

Cells were seeded on glass slides, fixed with 4% paraformaldehyde in PBS, and incubated overnight with the primary antibody at 4°C. Cells were then incubated with fluorescein- labeled goat anti-rabbit IgG and visualized by confocal microscopy.

3.1.7 Gene expression analysis.

RNA was extracted by using the TRIzol reagent from Invitrogen (Carlsbad, CA). Reverse transcription into cDNA was performed by using reverse transcriptase Superscript II and oligoDT from Invitrogen. Quantitative RT-PCR was performed with an ABI Prism 7000 thermal cycler from Applied Biosystems by using the SYBR green detection reagent. Cyclophilin was used as the housekeeping control gene.

3.1.8 GTT and ITT.

For the glucose tolerance test, mice received an intraperitoneal injection of D-glucose at 2 g/kg body weight after a 16-h fasting. For the insulin tolerance test, mice received an intraperitoneal injection of insulin at 0.5 unit/kg after a 6-h fasting.

3.1.9 Adenoviral expression vectors.

Adenoviruses expressing Hnf4 (Ad-Hnf4α), shRNA against Hnf4 (Ad-shHnf4α), or -galactosidase (Ad-shLacZ) were gifts from Yanqiao Zhang from the Northeast Ohio Medical University.

3.1.10 Cloning of SULT2B1b gene promoters, transient-transfection and reporter gene assays, and EMSA.

The mouse Sult2B1b gene promoter (nucleotides [nt] 156 to 200) and the human SULT2B1b gene promoter (nt 197 to 154) were cloned by PCR using the following primers (5= to 3=): Sult2B1b Forward, CGACGCGTCGCGGCAAAACTTGCAAAGTAA; Sult2B1b Reverse, GAAGATCTTCTCAGACGAGCTCC ACAGG; SULT2B1b Forward, CGACGCGTCGGCCATTTCCCAAATGAGCA; SULT2B1b Reverse, GAAGATCTTC GAGGACGAGCAGGGAGCA. The promoter sequences were then cloned into the pGL3-Luc reporter gene from Promega (Madison WI). Transient-transfection and luciferase reporter gene assays were performed as we have previously described, and the transfection efficiency was normalized against the -galactosidase activities from a cotransfected CMX- -galactosidase vector (6). EMSA using [32P] dCTP-labeled oligonucleotides and *in vitro*-translated proteins was carried out as we have previously described.

3.1.11 Stability assay of CS and TC in cells.

Primary hepatocytes were seeded onto 12-well plates and treated with vehicle, cholesterol sulfate (CS) (5 M), or thiocholesterol (TC) (5 M) for 0, 1, 2, 4, 8, 24, or 48 h. At the end of treatment, the medium was removed, 1 ml of methanol was added, and the cells were scraped and collected. The cells were sonicated for 15 s, and then 1 ml of dichloromethane was added. After vortexing for 1 min, the suspension was centrifuged at 13,600 rpm at 4°C for 20 min. The supernatant was transferred to a new tube and dried until analysis. For the detection of CS, the dried cellular extracts were reconstituted in 20 l of dichloromethane/methanol (1:1, vol/vol)

and diluted with 180 l of water-isopropanol-acetonitrile (2:5:3, vol/vol/vol). After centrifugation, 5 l of the supernatant was injected into the Waters ultraperformance liquid chromatography and quadrupole time of flight mass spectrometry (UPLC-QTOF MS) system for analysis. For the detection of TC, the cellular extracts were reconstituted in 20 l of dichloromethane and diluted with 180 l of acetonitrile. After centrifugation, 50 l of the supernatant was transferred to a new tube and 150 l of 0.1 M borate buffer (pH 8.0) was added. One hundred microliters of 10 mM monobromobimane in acetonitrile was added for derivatization. The mixture was gently shaken for 2 h before taking 10 l for the UPLC-QTOF MS analysis. Chromatographic separation was performed using an Acquity UPLC BEH C18 column (2.1 by 50 mm, 1.7 m; Waters Corporation, Milford, MA). For CS detection, the mobile phase A (MPA) was 10 mM ammonium acetate in water, and the mobile phase B (MPB) was 10 mM ammonium acetate in acetonitrile-water (95:5). The gradient began at 30% MPB and was held for 0.5 min, followed by 2.5 min of linear gradient to 95% MPB and holding for 3 min, and then decreased to 30% MPB for column equilibration. For TC detection, the MPA was 0.1% formic acid in water, and the MPB was 0.1% formic acid in acetonitrile. The gradient began at 30% MPB and was held for 0.5 min, followed by 2.5 min of linear gradient to 95% MPB and holding for 2.5 min, increased to 99% MPB in another 0.1 min, and held for 2.4 min and then decreased to 30% MPB for column equilibration. The flow rate of the mobile phase was 0.5 ml/min, and the column temperature was maintained at 50°C. The QTOF MS system was operated in a negative (for CS detection) or positive (for TC detection) high-resolution mode with electrospray ionization. The source and desolvation temperatures were set at 150 and 500°C, respectively. Nitrogen was applied as the cone gas (50 liters/h) and the desolvation gas (800 liters/h). Argon was applied as the collision gas. The capillary and cone voltages were

set at 0.8 kV and 40 V, respectively. QTOF MS was calibrated with sodium format and monitored by the intermittent injection of lock mass leucine encephalin (*m/z* 556.2771) in real time.

3.1.12 Statistical analysis.

Data are expressed as the means standard deviations (SD). One-way analysis of variance (ANOVA) Tukey's test or an unpaired Student *t* test was performed for statistical analysis using GraphPad Prism (San Diego, CA). *P* values of less than 0.05 were considered statistically significant.

3.1.13 Study approval.

The Central Animal Facility of the University of Pittsburgh is fully accredited by the American Association for Laboratory Animal Care (AALAC). All procedures were performed in accordance with relevant federal guidelines and with the approval of the University of Pittsburgh ethical committee.

3.2 RESULTS

3.2.1 HNF4α positively regulates the expression of Sult2B1b in mouse primary hepatocytes and in mouse liver.

We have previously reported that SULT2B1b can negatively regulate the activity of HNF4α (6). To our surprise, we found that the expression of SULT2B1b was positively regulated by HNF4α . In the gain-of-function models, infection of primary mouse hepatocytes with adenovirus expressing Hnf4 α (Ad-Hnf4α) resulted in the mRNA induction of *Sult2B1b*, as well as the known HNF4α target genes *G6pase* and *Pepck* (Fig. 1A). The overexpression of Hnf4α and induction Sult2B1b were verified at the protein level by Western blotting (Fig. 1B). In a pharmacological gain-of-function model, treatment of primary hepatocytes with linoleic acid, an endogenous Hnf4α activator (74), induced the expression of *Sult2B1b*, *G6pase*, and *Pepck* (Fig. 1C). The induction of *Sult2B1b* by linoleic acid was abolished when the expression of Hnf4α was downregulated by short hairpin RNA (shRNA) (Fig. 1D). Downregulation of Hnf4α also decreased the basal expression of *Sult2B1b*, *G6pase*, and *Pepck* (Fig. 1D). The shRNA knockdown of Hnf4α and downregulation of Sult2B1b were verified at the protein level by Western blotting (Fig. 1F). In a pharmacological loss-of- function model, treatment of primary mouse hepatocytes with BIM5078, an inhibitor of HNF4α (75), downregulated the expression of *Sult2B1b*, *G6pase*, and *Pepck* (Fig. 1G). *In vivo*, hydrodynamic transfection of the mouse liver with the Hnf4α expression vector increased the hepatic expression of Sult2B1b at both the mRNA (Fig. 1H) and the protein (Fig. 1I) levels.

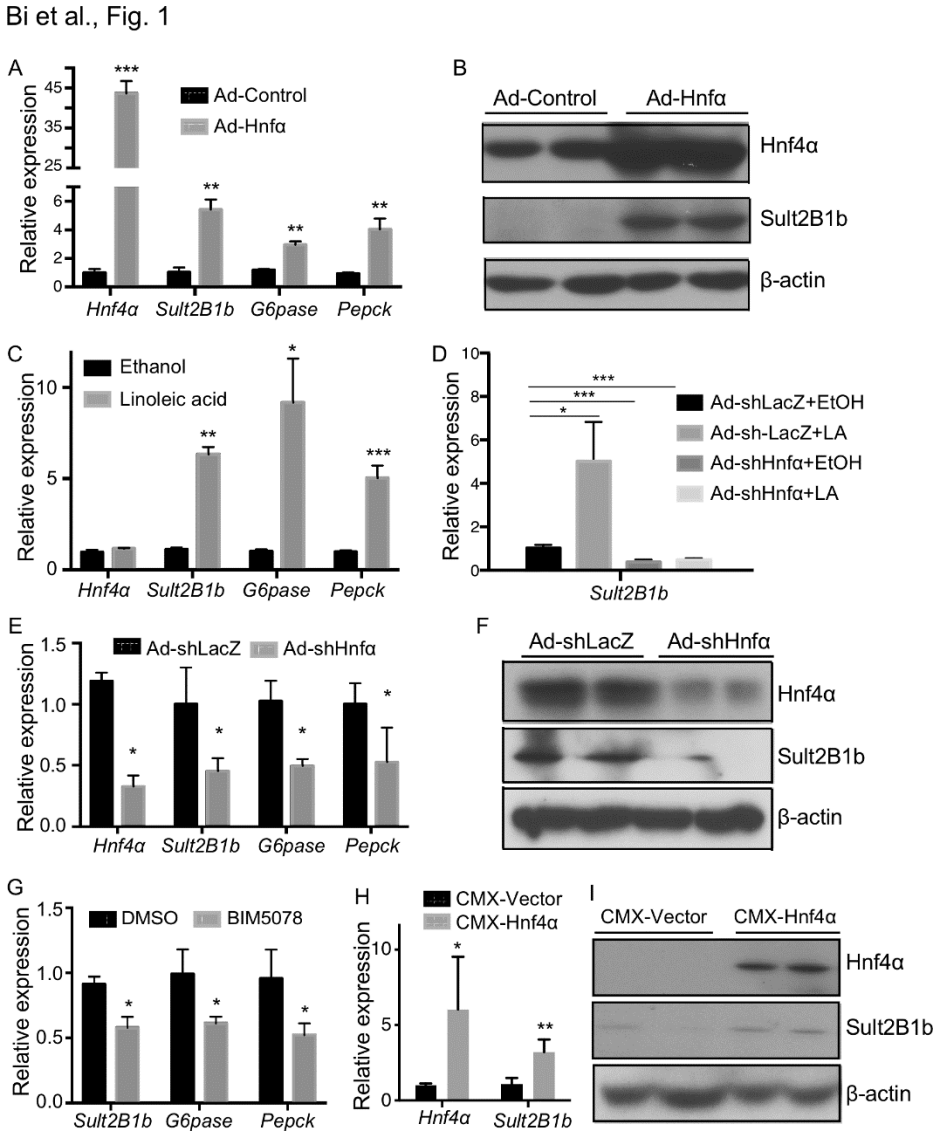

Figure 1. HNF4α positively regulates the expression of Sult2B1b in mouse primary hepatocytes and in mouse liver.

(A to G) Experiments were conducted using primary hepatocytes isolated from 8-week-old WT male mice. (A) Relative mRNA expression of *Hnf4α* , *Sult2B1b*, *G6pase*, and *Pepck* in hepatocytes infected with adenovirus encoding Hnf4α or the control virus as measured by real-time PCR. The expression of each gene was arbitrarily set as 1 in hepatocytes infected with the control virus. (B) Cells were the same as described for panel A. The protein expression of Hnf4α and Sult2B1b was measured by Western blotting. (C) Relative mRNA expression of *Hnf4α*, *Sult2B1b*, *G6pase*, and *Pepck* in hepatocytes treated with the ethanol control or linoleic acid (25 M) for 24 h. The expression of each gene was arbitrarily set as 1 in cells treated with ethanol. (D)

Hepatocytes were first infected with adenovirus encoding shHnf4α or the control virus for 24 h before being treated with ethanol or linoleic acid (25 M) for another 24 h. The expression of *Sult2B1b* was measured by real-time PCR. (E and F) Hepatocytes were first infected with adenovirus encoding shHnf4α or the control virus for 24 h, and the gene expression was evaluated by real-time PCR (E) and Western blotting (F), respectively. (G) Relative mRNA expression of *Sult2B1b*, *G6pase*, and *Pepck* in hepatocytes treated with vehicle (dimethyl sulfoxide [DMSO]) or the Hnf4α inhibitor BIM5078 (20 M) for 24 h. (H and I) Eight-week-old WT male mouse livers were hydrodynamically transfected with the empty vector or the pCMX-Hnf4α expression plasmid. The hepatic expressions of Hnf4α and Sult2B1b mRNA (H) and protein (I) were measured by real-time PCR and Western blotting, respectively. Results are expressed as means SD from three independent experiments (5 mice per group). *, *P* 0.05; **, *P* 0.01; ***, *P* 0.001.

3.2.2 HNF4α induces the expression of SULT2B1b in human liver cells

The positive regulation of SULT2B1b by HNF4α is conserved in human liver cells. In the human hepatoma HepG2 cells, transfection with the HNF4α expression vector increased the expression of SULT2B1b (Fig. 2A). In human primary hepatocytes (HPH), treatment of cells with the HNF4α activator linoleic acid induced the expression of both SULT2B1b and G6Pase (Fig. 2B). In contrast, the basal mRNA expression of SULT2B1b and G6Pase was decreased when the expression of HNF4α was knocked down by shRNA (Fig. 2C). The shRNA knockdown of HNF4α and downregulation of SULT2B1b in human primary hepatocytes were verified at the protein level by Western blotting (Fig. 2D). The basal expression levels of SULT2B1b and G6Pase were decreased in human primary hepatocytes treated with the HNF4α inhibitor BIM5078 (Fig. 2E).

Bi et al., Fig. 2

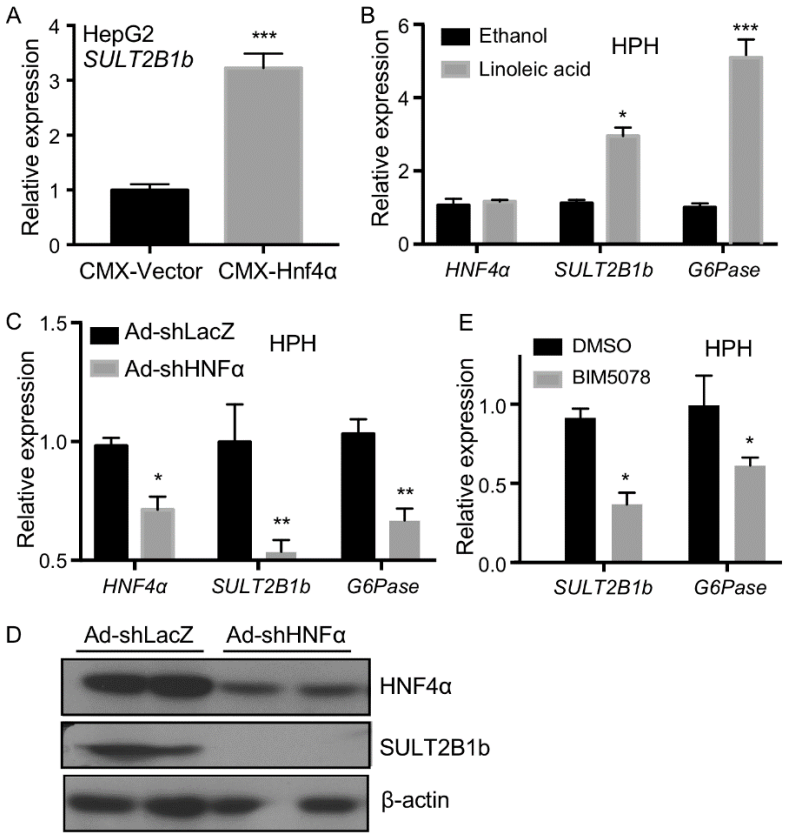

Figure 2 HNF4α induces the expression of SULT2B1b in human liver cells.

(A) Relative mRNA expression of *SULT2B1b* in HepG2 cells transfected with the empty vector or the Hnf4α -expressing plasmid. The expression of each gene was arbitrarily set as 1 in cells transfected with the empty vector. (B) Relative mRNA expression of *HNF4α*, *SULT2B1b*, and *G6Pase* in human primary hepatocytes (HPH) treated with ethanol or linoleic acid (25 M) for 24 h. The expression of each gene was arbitrarily set as 1 in cells treated with ethanol. (C) mRNA expression of *HNF4α*, *SULT2B1b*, and *G6Pase* in HPH infected with adenovirus encoding shHNF4α or the control virus. The expression of each gene was arbitrarily set as 1 in cells infected with the control virus. (D) Cells were the same as described for panel C. The protein expression of HNF4α and SULT2B1b was measured by Western blotting. (E) Relative mRNA expression of *SULT2B1b* and *G6Pase* in HPH treated with the vehicle (DMSO) or the HNF4α inhibitor BIM5078 (20 M) for 24 h. The expression of each gene was arbitrarily set as 1 in cells treated with DMSO. Results are expressed as means SD from three independent experiments. *, *P* 0.05; **, *P* 0.01; ***, *P* 0.001.

3.2.3 The mouse and human SULT2B1b genes are transcriptional targets of HNF4α.

The regulation of mouse and human SULT2B1b by HNF4α strongly suggested that the SULT2B1b gene is a direct transcriptional target of HNF4α . As a transcriptional factor, HNF4α often regulates gene expression by binding to the promoter regions of its target genes (76). Bioinformatic inspection of the mouse and human SULT2B1b gene promoters revealed a putative HNF4α binding site on each of the promoter (Fig. 3A, top panel). The binding of HNF4α to these two putative sites was confirmed by electrophoretic mobility shift assay (EMSA) (Fig. 3A, bottom panel). The binding was specific in that the binding was efficiently competed by unlabeled wild-type (WT) binding sites ("self"), but not by their mutant variants. The recruitment of HNF4α to the mouse *Sult2B1b* gene promoter was confirmed by chromatin immunoprecipitation (ChIP) assay on mouse primary hepatocytes (Fig. 3B), in which the recruitment of Hnf4α to its known binding site in the *Pepck* gene promoter and a distal region in the *Sult2B1b* gene promoter were included as the positive and negative controls, respectively (Fig. 3B). The recruitment of HNF4α to the human *SULT2B1b* gene promoter was confirmed by ChIP assay on human primary hepatocytes (Fig. 3C). To determine whether the mouse and human *SULT2B1b* gene promoters can be transactivated by HNF4α and the functional relevance of the HNF4α binding sites, we cloned the mouse and human *SULT2B1b* gene promoters, as well as their mutant variants in which the HNF4α binding sites were mutated by site-directed mutagenesis. Both the mouse (Fig. 3D) and human (Fig. 3E) *SULT2B1b* gene promoter luciferase reporter genes were activated by the of the HNF4α binding sites, we cloned the mouse and human *SULT2B1b* gene promoters, as well as their mutant variants in which the HNF4α binding sites were mutated by site-directed mutagenesis. Both the mouse (Fig. 3D) and human (Fig. 3E) *SULT2B1b* gene promoter luciferase reporter genes

were activated by the cotransfection of HNF4α , but the activation was abolished when the HNF4α binding sites were mutated.

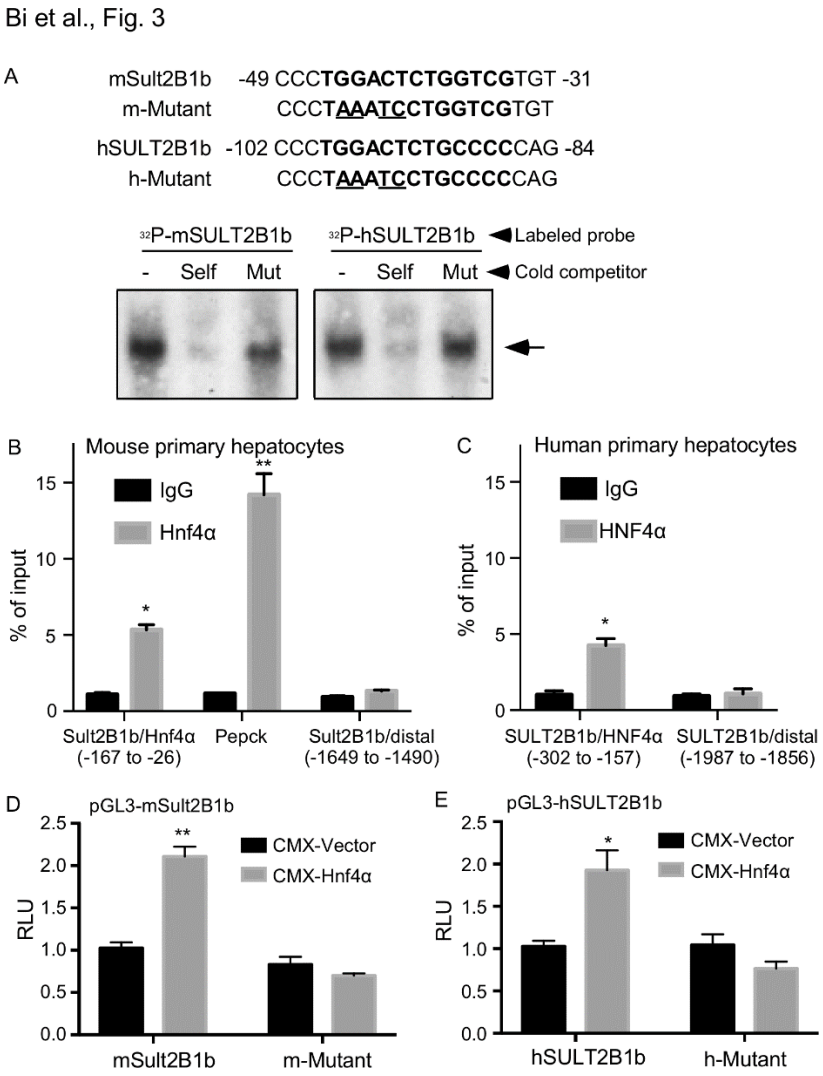

Figure 3 The mouse and human *SULT2B1b* genes are transcriptional targets of HNF4α.

(A) Sequences of the predicted HNF4α binding sites in the mouse and human *SULT2B1b* gene promoters and their mutant variants (top). The bindings of HNF4α to the putative HNF4α binding sites were shown by electrophoretic mobility shift assay (EMSA) (bottom). (B and C) ChIP assay showing the recruitment of HNF4α onto the mouse (C) and human (D) SULT2B1b

gene promoters. (D and E) Activation of the mouse (D) and human (E) SULT2B1b promoter reporter genes by HNF4α. Cells were cotransfected with the indicated WT or mutant reporter genes, and receptors were monitored by luciferase assay. Results are expressed as means SD from three independent experiments. *, *P* 0.05; **, *P* 0.01.

3.2.4 Downregulation or ablation of Sult2B1b increases the gluconeogenic activity of Hnf4α in mouse primary hepatocytes.

Having shown that SULT2B1b is an HNF4α target gene and knowing that SULT2B1b can inhibit the gluconeogenic activity of HNF4α , we hypothesized that the induction of SULT2B1b by HNF4α may represent a negative feedback to limit the gluconeogenic activity of HNF4α . Based on this hypothesis, we predicted that downregulation or ablation of SULT2B1b will increase the gluconeogenic activity of HNF4α due to the lack of SULT2B1b-mediated inhibition. We first tested our hypothesis *in vitro* using mouse primary hepatocytes. In this experiment, hepatocytes were transiently transfected with the Sult2B1b-targeting small interfering RNA (siRNA) or the nontargeting control siRNA, in the presence or absence of the cotransfection of HNF4α , followed by the measurement of forskolin (FSK)-responsive glucose production and the expression of gluconeogenic genes. The knockdown of *Sult2B1b* (Fig. 4A) and overexpression of *Hnf4α* (Fig. 4B) were confirmed by real-time PCR (RT-PCR). As shown in Fig. 4C, knockdown of Sult2B1b increased the basal and Hnf4α -responsive glucose production, which was accompanied by increased expression of *G6pase* (Fig. 4D) and *Pepck* (Fig. 4E). In another independent loss-of-function model, we infected hepatocytes isolated from the WT and Sult2B1b$^{-/-}$ mice with control adenovirus (Ad-Control) or Ad-Hnf4α . The expression of transduced *Hnf4α* was verified by real-time PCR (Fig. 4F). Again, increased Hnf4α -responsive glucose production (Fig. 4G) and

expression of *G6pase* (Fig. 4H) and *Pepck* (Fig. 4I) were observed in Sult2B1b$^{-/-}$ hepatocytes compared to what was seen in hepatocytes isolated from the WT mice.

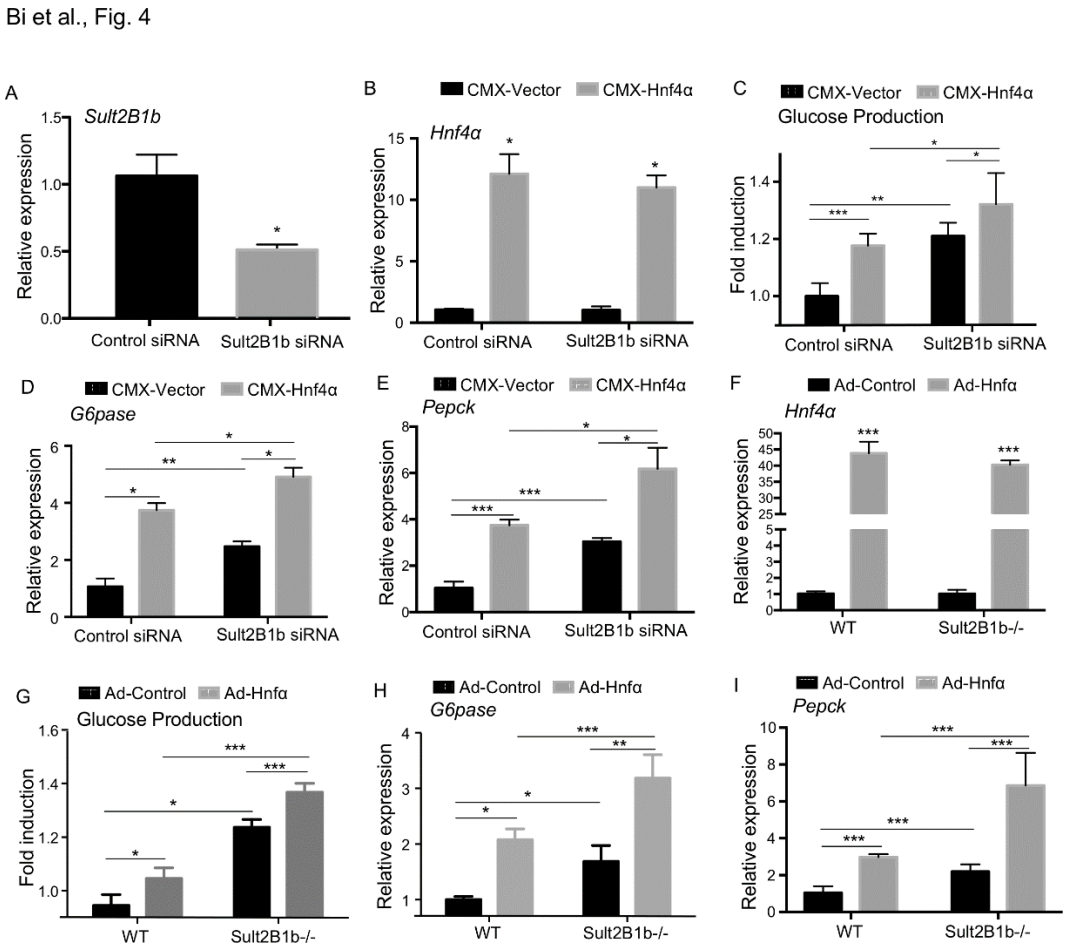

Figure 4 Downregulation or ablation of Sult2B1b increases the gluconeogenic activity of Hnf4α in mouse primary hepatocytes.

(A) Hepatocytes isolated from 8-week-old WT male mice were transfected with scrambled or Sult2B1b-targeting siRNA for 48 h. The downregulation of *Sult2B1b* was verified by real-time PCR. The expression was arbitrarily set as 1 in cells transfected with scrambled siRNA. (B to E) Relative mRNA expression of *Hnf4α* (B), *G6pase* (D), and *Pepck* (E) and glucose production (C) in hepatocytes transfected with scrambled or Sult2B1b-targeting siRNA for 24 h followed by transfection with the empty vector or the pCMX-Hnf4α -expressing vector for another 24 h. The expression of each gene or glucose production was arbitrarily set as 1 in cells transfected with scrambled siRNA followed by transfection with the empty vector. (F to I) Relative mRNA expression of *Hnf4α* (F), *G6pase* (H), and *Pepck* (I) and glucose production (G) in hepatocytes isolated from 8-week-old male WT or Sult2B1b$^{-/-}$ mice infected with adenovirus encoding Hnf4α

or the control virus. The expression of each gene or glucose production was arbitrarily set as 1 in cells isolated from WT mice infected with the control virus. Results are expressed as means SD from three independent experiments. *, *P* 0.05; **, *P* 0.01; ***, *P* 0.001.

3.2.5 Ablation of Sult2B1b increases the gluconeogenic activity of Hnf4α *in vivo*, and Sult2B1b$^{-/-}$ mice exhibit elevated fasting blood glucose levels.

To determine the effect of Sult2B1b ablation on Hnf4α activity *in vivo*, WT and Sult2B1b$^{-/-}$ mice were hydrodynamically transfected with the empty vector or the Hnf4α expression vector. The overexpression of *Hnf4α* in both genotypes was confirmed by real-time PCR (Fig. 5A). The Sult2B1b$^{-/-}$ mice showed increased basal and Hnf4α -responsive expression of *G6pase* (Fig. 5B) and *Pepck* (Fig. 5C).

Fasting is known to induce the expression and activity of Hnf4α and increase gluconeogenesis (9). To determine the effect of Sult2B1b ablation on fasting-responsive gluconeogenesis, WT and Sult2B1b$^{-/-}$ mice maintained on a chow diet were fasted for 24 h. As shown in Fig. 5D, fasting induced the expression of *Hnf4α* in both genotypes. The induction of Hnf4α in WT mice was accompanied by the induction of *Sult2B1b* (Fig. 5E), consistent with the notion that Sult2B1b is a transcriptional target of Hnf4α . The fasting-responsive induction of Hnf4α and Sult2B1b protein expression was verified by Western blotting (Fig. 5F). The fasting-responsive expression of *G6pase* (Fig. 5G), but not of *Pepck* (Fig. 5H), was elevated in Sult2B1b$^{-/-}$ mice compared to their WT counter- parts. Moreover, the Sult2B1b$^{-/-}$ mice exhibited higher levels of fasting glucose (Fig. 5I), which may have been contributed to by the increased gluconeogenesis.

Bi et al., Fig. 5

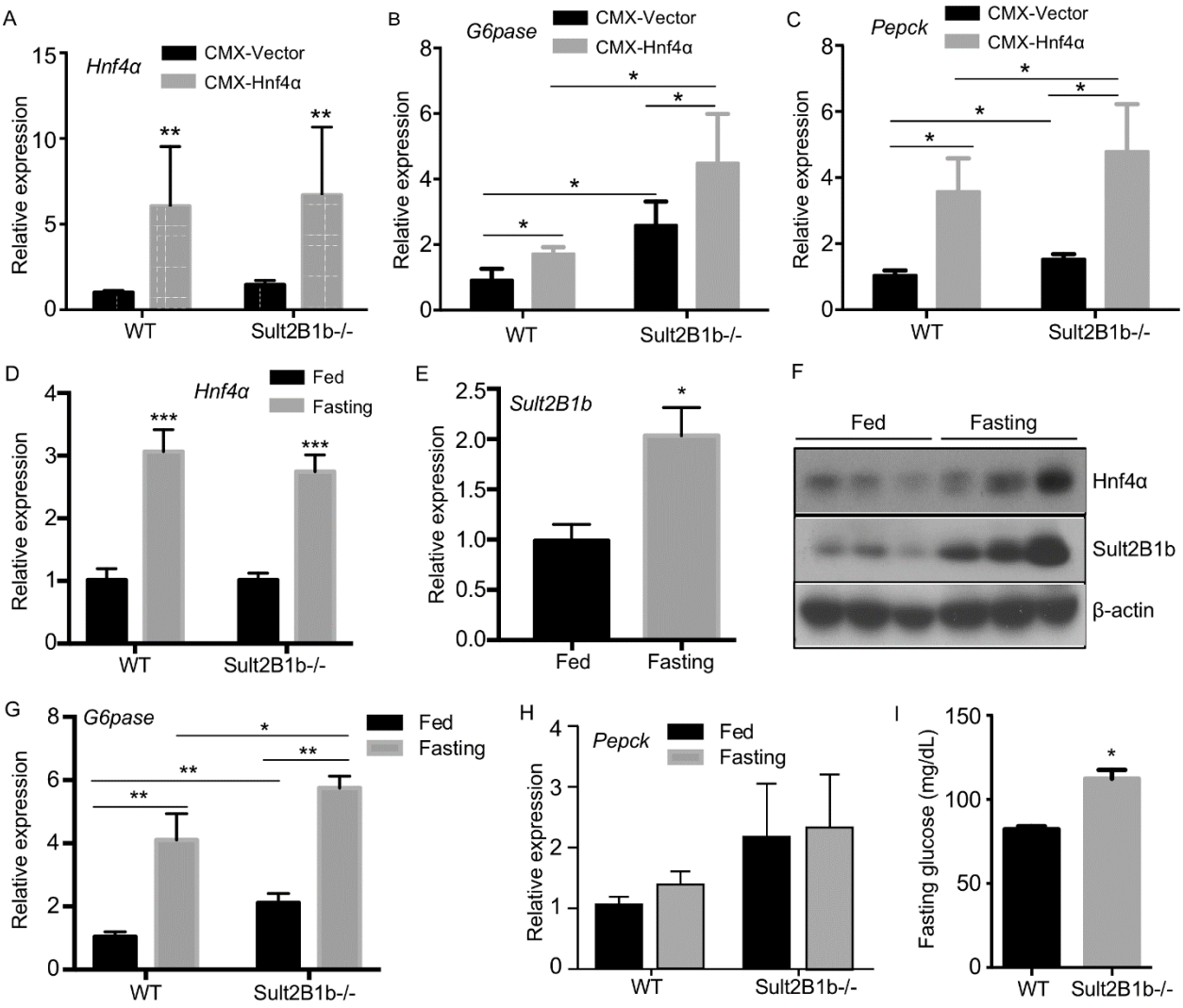

Figure 5 Ablation of Sult2B1b increases the gluconeogenic activity of Hnf4α *in vivo*, and Sult2B1b$^{-/-}$ mice exhibit elevated fasting blood glucose levels.

Eight-week-old WT and Sult2B1b$^{-/-}$ male mice were used. (A to C) Relative hepatic mRNA expression of *Hnf4α* (A), *G6pase* (B), and *Pepck* (C) in the livers of WT and Sult2B1b$^{-/-}$ mice hydrodynamically transfected with the empty vector or the Hnf4α -expressing vector. The expression of each gene was arbitrarily set as 1 in mice transfected with the empty vector. (D to H) Relative hepatic expressions of *Hnf4α* (D), *Sult2B1b* (E), Hnf4α and Sult2B1b (F), *G6pase* (G), and *Pepck* (H) in fed and fasted WT and Sult2B1b$^{-/-}$ mice were measured by real-time PCR

(D, E, G, and H) or Western blotting (F). The expression of each gene was arbitrarily set as 1 in fed WT mice. (I) Fasting glucose levels. *n* 5 mice per group. *, *P* 0.05; **, *P* 0.01; ***, *P* 0.001.

3.2.6 Ablation of Sult2B1b increases the acetylation of Hnf4α by suppressing the Hnf4α deacetylase Sirt1.

The transcriptional activity of HNF4α can be regulated by acetylation. Acetylation of HNF4α activates HNF4α by promoting its nuclear translocation (6 and 12). We first used immunofluorescence to determine whether Sult2B1b ablation impacted the subcellular localization of Hnf4α in primary mouse hepatocytes. Indeed, compared to the WT hepatocytes, in which Hnf4α was distributed in both the cytoplasm and nucleus, Hnf4α was almost exclusively nuclear in hepatocytes isolated from the Sult2B1b$^{-/-}$ mice (Fig. 6A). The effect of Sult2B1b ablation on the subcellular distribution of Hnf4α was further confirmed by nuclear-cytosolic fractionation of the liver and Western blotting (Fig. 6B). To examine the effect of Sult2B1b ablation on the acetylation of Hnf4α , hepatocyte lysates were immunoprecipitated with an anti-acetyl lysine antibody before immunoblotting with an anti-Hnf4α antibody. As shown in Fig. 6C, the acetylation of Hnf4α was increased in hepatocytes isolated from the Sult2B1b$^{-/-}$ mice. The increased acetylation of Hnf4α in Sult2B1b$^{-/-}$ mice was associated with a decreased expression of Sirt1, a NAD (+)-dependent deacetylase that can deacetylate HNF4α (13) (Fig. 6D), as well as an increased expression of acetyl coenzyme A (acetyl-CoA) synthetase (Acss) (Fig. 6E), the enzyme that catalyzes the formation of the acetyl donor acetyl-CoA (77).

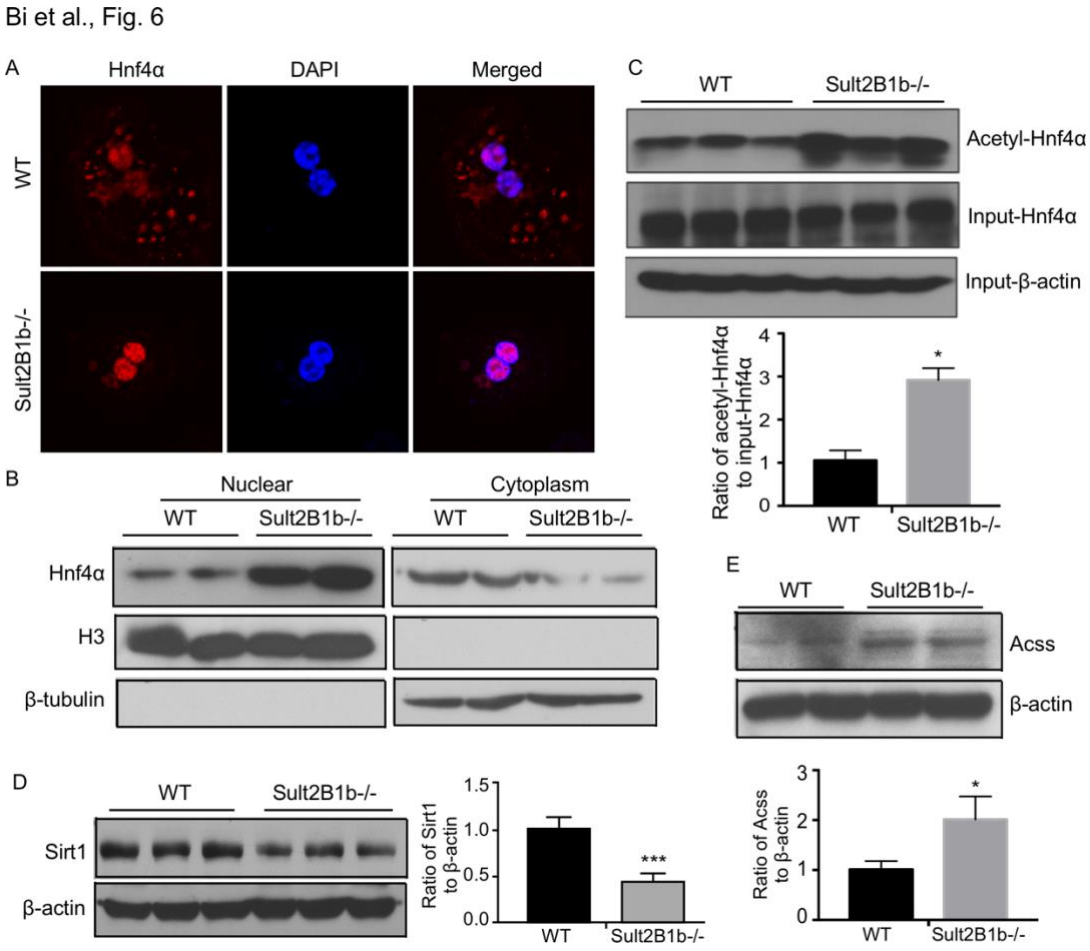

Figure 6 Ablation of Sult2B1b increases the acetylation of Hnf4α by suppressing the Hnf4α deacetylase Sirt1. Eight-week-old WT and Sult2B1b$^{-/-}$ male mice were used.

(A) The subcellular distribution of Hnf4α was visualized by immunofluorescence using an anti-Hnf4α antibody (red) in primary hepatocytes isolated from WT and Sult2B1b$^{-/-}$ mice. DAPI (4=,6-diamidino-2-phenylindole; blue) was used for nuclear counterstaining. (B) Western blot analysis of the Hnf4α protein levels in the nuclear and cytoplasmic fractions of WT and Sult2B1b$^{-/-}$ mouse liver. The purity of the nuclear and cytoplasmic fractions was confirmed by immunoblotting with histon-H3 antibody (a nuclear marker) and -tubulin antibody (a cytoplasmic marker), respectively. (C) Liver lysates of WT and Sult2B1b$^{-/-}$ mice were immunoprecipitated with an anti-acetyl lysine antibody before immunoblotting with an anti-Hnf4α antibody. Shown below the blot is the densitometric quantification of the Western blotting results. (D and E) The hepatic expression levels of Sirt1 (D) and Acss (E) proteins were measured by Western blotting. Shown on the right of (D) or below (E) the blot is the densitometric quantification of the Western blotting results. Results are expressed as means SD. *, *P* 0.05.

3.2.7 Thiocholesterol shows an improved intracellular stability and better efficacy in inhibiting gluconeogenesis in primary hepatocytes.

We previously reported that CS can inhibit Hnf4α -mediated gluconeogenesis, which is an integral component of Hnf4α - and Sult2B1b-mediated negative feedback regulation of gluconeogenesis. However, CS is readily hydrolyzed by the steroid sulfatase, limiting its utility as a therapeutic agent (72). We then synthesized thiocholesterol (TC), a structural analog of CS generated by replacing the sulfate with a thiol group that is predicted to be hydrolysis resistant (Fig. 7A). We hypothesized that TC may mimic the antigluconeogenic activity of CS but with a superior bioavailability due to its resistance to hydrolysis. To compare the intracellular stability of TC and CS, mouse primary hepatocytes were treated with 5 M TC or CS, and their intracellular concentrations were monitored over a 48-h period. As shown in Fig. 7B, in CS-treated cells, the intracellular concentration of CS peaked at 4 h but declined steadily thereafter, reaching a very low level after 24 h. In contrast, the intracellular concentration of TC continued rising until 48 h after the drug treatment. At the functional level, treatment of mouse primary hepatocytes with 5 M TC, but not 5 M CS, was effective in reducing FSK-stimulated glucose production (Fig. 7C) and inhibiting the expression of *G6pase* and *Pepck* (Fig. 7D). CS at 20 M could achieve an inhibitory effect similar to that obtained with 5M TC (Fig. 7C and D). A similar pattern of superior inhibitory effects of TC on glucose production (Fig. 7E) and gluconeogenic gene expression (Fig. 7F) was observed in human primary hepatocytes. Thiocholesterol was also more efficient than CS in inducing the nuclear exclusion of Hnf4α in mouse primary hepatocytes as shown by immunofluorescence (Fig. 7G) and nuclear-cytosolic fractionation of the hepatocytes and Western

blotting (Fig. 7H). Neither TC nor CS affected the mRNA expression of *Hnf4α* in mouse primary hepatocytes as measured by real-time (RT) PCR (data not shown).

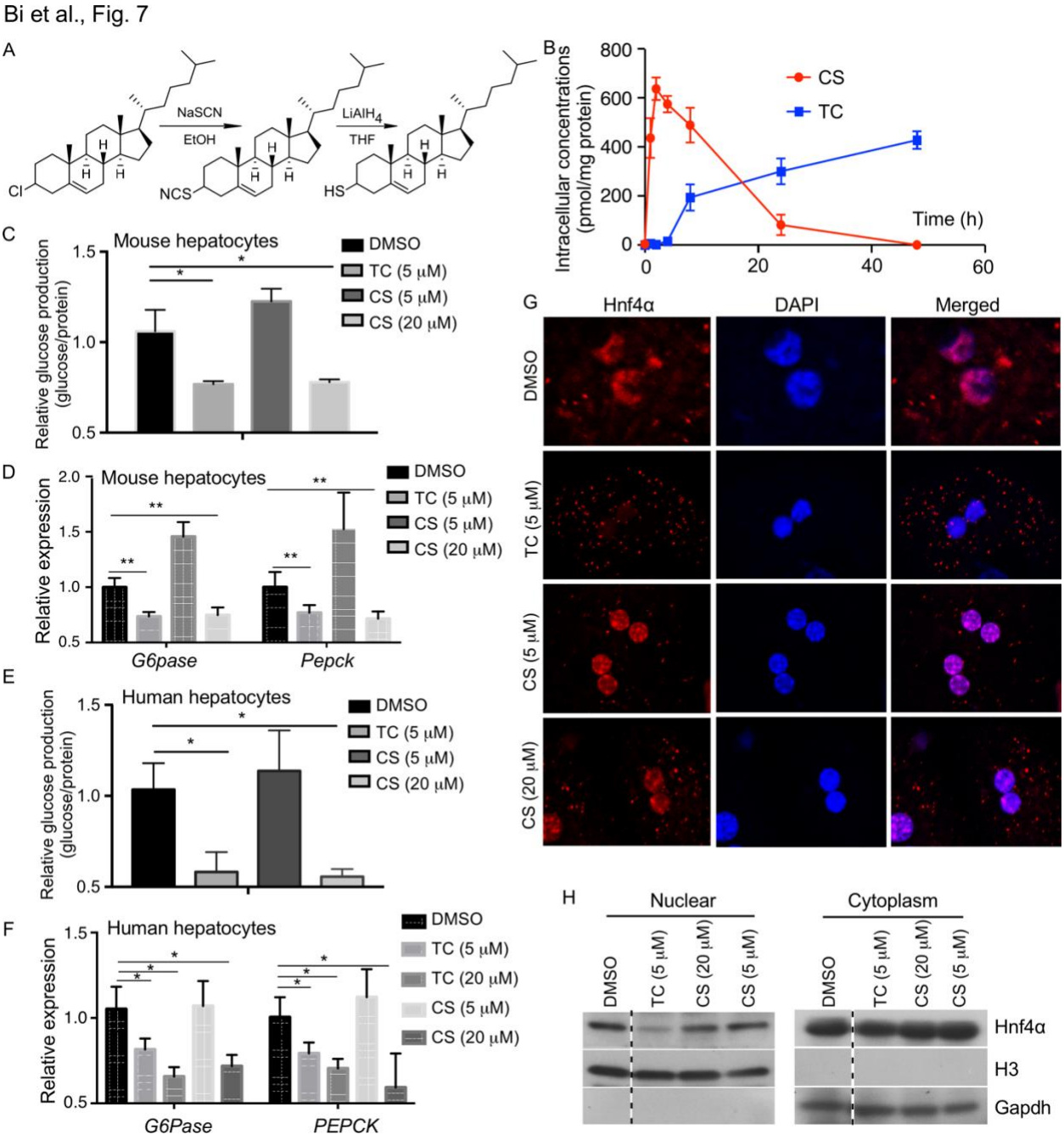

Figure 7 Thiocholesterol (TC) shows an improved intracellular stability and better efficacy in inhibiting gluconeogenesis in primary hepatocytes.

(A) Schematic depiction of the synthesis of TC from cholesteryl chloride. (B) Mouse primary hepatocytes isolated from 8-week-old male WT mice were treated with 5 M TC or CS for up to 48 h, and the intracellular concentrations of TC and CS were measured by using UPLC-mass spectrometry. (C and D) Glucose production (C) and expression of gluconeogenic genes (D) in mouse primary hepatocytes treated with the indicated concentrations of drugs for 24 h. Cells were treated with 10 M FSK for 2.5 h before the glucose production assay. The expression of each gene or glucose production was arbitrarily set as 1 in cells treated with DMSO. (E and F) The designs of the experiments were similar to those described for panels C and D, except that human primary hepatocytes were used. (G) The subcellular distribution of Hnf4α was visualized by immunofluorescence using an anti-Hnf4α antibody (red) in primary hepatocytes isolated from WT mice and treated with the indicated concentrations of drugs. DAPI (blue) was used for nuclear counterstaining. (H) The subcellular distribution of Hnf4α was measured by nuclear-cytosolic fractionation of the hepatocytes and Western blotting. Histon-H3 and glyceraldehyde-3-phosphate dehydrogenase (Gapdh) are nuclear and cytoplasmic markers, respectively. All four lanes are from the same blot, with the dotted lines indicating noncontinuous lanes. Results are expressed as means SD. *, *P* 0.05; **, *P* 0.01.

3.2.8 Thiocholesterol exhibits a superior activity in reducing fasting blood glucose level and improving overall glucose homeostasis in HFD-fed mice.

We have previously reported that treatment of HFD-fed mice with CS can inhibit gluconeogenesis and improve insulin sensitivity (6). We then used the same HFD model to determine whether TC was more efficacious than CS in improving the overall glucose homeostasis. Mice were fed with HFD for 12 weeks before receiving intraperitoneal (i.p.) doses of TC or CS at 25 mg/kg of body weight 3 times per week for 2 weeks. At 24 h after the last dose of drug treatment, TC was more effective than CS in lowering the fasting blood glucose level (Fig. 8A). At 48 h after the last drug dose, TC remained effective in reducing the fasting blood glucose level, but CS was no longer effective (Fig. 8A). Thiocholesterol was also more effective than CS in reducing the gluconeogenic (Fig. 8B) and lipogenic (Fig. 8C) gene expression levels. Treatment with TC was more effective in improving the animal's performance in the glucose tolerance test

(GTT) (Fig. 8D) and insulin tolerance test (ITT) (Fig. 8E), attenuating HFD-induced hepatic steatosis as shown by Oil red O staining (Fig. 8F) and lowering the serum triglyceride and cholesterol levels (Fig. 8G) without affecting the plasma insulin levels (data not shown). Treatment with TC was also effective in inducing the protein expression of Sirt1 (Fig. 8H) and suppressing the protein expression of Acss (Fig. 8I). This regimen of TC or CS was not toxic to the mice, because they did not elevate the activities of ALT and AST, nor did they affect the animal's food intake and body weight (data not shown). Treatment with TC or CS had little effect on the hepatic mRNA expression of *Hnf4α in vivo* (data not shown).

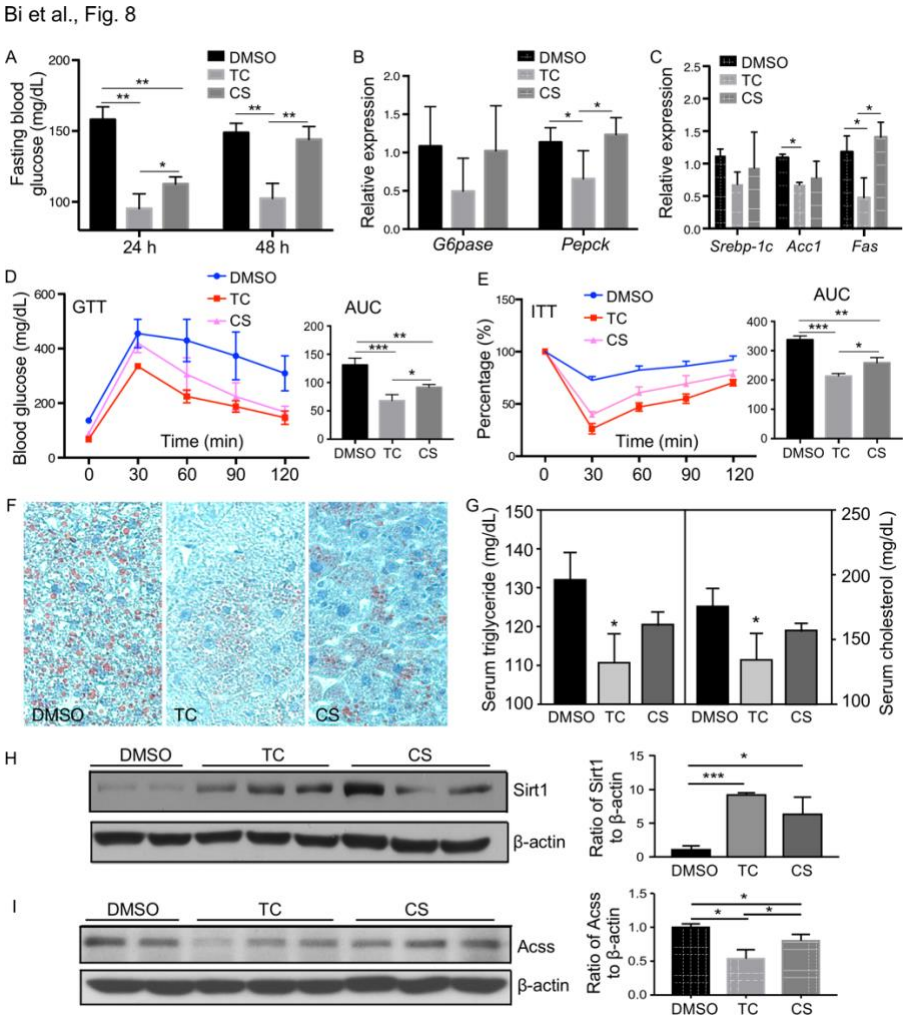

Figure 8 Thiocholesterol exhibits a superior activity in reducing fasting blood glucose level and improving overall glucose homeostasis in HFD-fed mice.

Six-week-old WT C56BL/6 male mice were fed a high-fat diet (HFD) for 12 weeks followed by i.p. injections of vehicle (DMSO), TC (25 mg/kg), or CS (25 mg/kg) 3 times per week for 2 weeks while the mice remained on HFD. (A) Fasting blood glucose levels 24 h or 48 h after the last dose of drugs. Mice were fasted for 6 h before the blood glucose tests. (B and C) Hepatic expression of gluconeogenic genes (B) and lipogenic genes (C) 3 days after the last dose of drugs was measured by real-time PCR. The expression of each gene was arbitrarily set as 1 in mice treated with DMSO. (D and E) Shown on the right of each panel are the quantifications of GTT (D) and ITT (E) presented as areas under the curve (AUC). (F and G) Oil red O staining of the liver sections (F) and serum triglyceride and cholesterol levels (G). (H and I) Hepatic expression levels of the Sirt1 (H) and Acss (I) proteins was measured by Western blotting. Shown on the right are the densitometric quantifications of the Western blotting. Results are expressed as means SD from three independent experiments (5 mice per group). *, *P* 0.05; **, *P* 0.01; ***, *P* 0.001.

3.3 DISCUSSION

SULT2B1b catalyzes the sulfoconjugation of cholesterol to synthesize CS. We have previously shown that the expression of SULT2B1b in the liver was induced in diabetic obese mice and during the fasting-to-fed transition. We went on to show that SULT2B1b and CS inhibited gluconeogenesis by targeting HNF4α in both cell cultures and transgenic mice (6). These results suggested that the induction of SULT2B1b may represent a protective response to metabolic stresses.

Knowing that SULT2B1b is a negative regulator of HNF4α, it was interesting and intriguing to find that SULT2B1b itself is a transcriptional target of HNF4α. HNF4α is a transcriptional factor of diverse functions, including its gluconeogenic activity by regulating the key gluconeogenic enzymes. Although hepatic gluconeogenesis is an essential cellular function, uncontrolled gluconeogenesis can be pathogenic, including the development of T2D (7–11).

Indeed, genetic variants of HNF4α have been associated with an increased risk of T2D and metabolic syndrome in humans (78 and 79). Therefore, it is necessary to have a cellular mechanism to limit gluconeogenesis, including that mediated by HNF4α. Based on our results, we propose that the positive regulation of SULT2B1b by HNF4α represents an effective cellular mechanism to keep the HNF4α-mediated gluconeogenesis in check, including in the context of fasting response.

Consistent with our hypothesis, knockdown or knockout of Sult2B1b enhanced the gluconeogenic activity of HNF4α, which was associated with increased acetylation and nuclear enrichment of HNF4α. The increased acetylation of HNF4α may have accounted for the nuclear enrichment of HNF4α, because acetylation prevents the active export of HNF4α to the cytoplasm and increases the DNA binding of HNF4α (12, 14). The increased acetylation of HNF4α in Sult2B1b$^{-/-}$ hepatocytes may be explained by the combined effects of a decreased expression of the HNF4α deacetylase Sirt1 and an increased expression of the acetyl-CoA-generating enzyme Acss. The mechanisms by which Sirt 1 and Acss are regulated by Sult2B1b remain to be understood. CBP/p300 has been shown to acetylate HNF4α (14), but the expression of CBP/p300 was not affected in the Sult2B1b$^{-/-}$ hepatocytes (data not shown).

In addition to inhibiting gluconeogenesis, SULT2B1b has been reported to have many other functions in different cell types and tissues, ranging from inhibiting lipogenesis to promoting the liver cell proliferation (80), affecting prostate and colorectal cancer cells (81), and inhibiting the T cell receptor signaling (82). It remains to be determined whether HNF4α, as a positive regulator of SULT2B1b, is also involved in these additional functions of SULT2B1b. Meanwhile,

HNF4α is a transcriptional factor that has numerous functions beyond promoting gluconeogenesis (83). It would be interesting to know whether and how SULT2B1b, as an HNF4α target gene, may have contributed to other cellular functions of HNF4α.

Dysregulated gluconeogenesis is primarily responsible for the increased hepatic glucose production in T2D (11), suggesting that targeting the gluconeogenic pathway could attenuate hyperglycemia. Indeed, metformin, one of the most prescribed drugs for T2D, is believed to exert its therapeutic benefit by reducing hepatic gluconeogenesis (84). Based on our findings, it is tempting to explore CS as a potential therapeutic agent to manage metabolic disorders, because it is a key component in the HNF4α - SULT2B1b negative feedback regulation of gluconeogenesis. However, the natural CS is chemically unstable, because it is readily hydrolyzed by the steroid sulfatase. In addressing the chemical instability of CS, we have developed and characterized TC, a hydrolysis-resistant derivative of CS. Our results showed that TC was superior to CS in inhibiting gluconeogenesis and improving overall glucose homeostasis in diabetic mice, which was attributed to the increased stability and bioavailability of TC. Certain cholesterol derivatives such as oxysterols have been shown to activate LXR, but neither TC nor CS affected the activity of LXR in reporter gene assays (data not shown).

In summary, we have identified the cholesterol sulfotransferase SULT2B1b as a novel transcript target of HNF4α. The induction of SULT2B1b by HNF4α constitutes a negative feedback mechanism to prevent uncontrolled gluconeogenesis in diabetes or fasting response. As a structural and functional analog of CS, the hydrolysis-resistant TC may be further explored as a therapeutic agent to inhibit gluconeogenesis and manage hyperglycemia (PIC. 2).

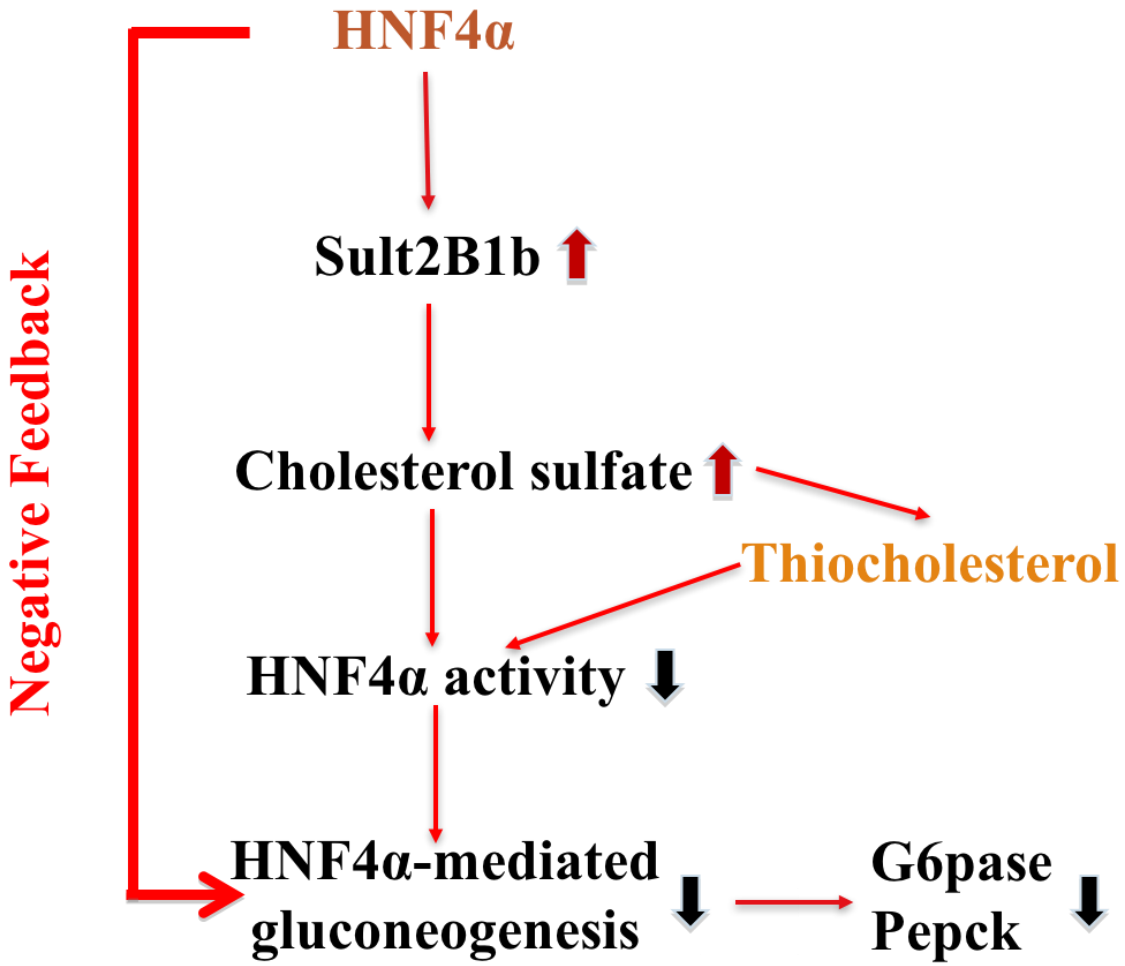

Picture 2 Scaffold of negative feedback regulation between HNF4α and SULT2B1b and its enzymatic product CS and derivative TC to regulate hepatic gluconeogenesis.

4.0 CHAPTER IV: ADIPOSE TISSUE- AND SEX-SPECIFIC ROLE OF STEROID SULFATASE IN EBERGY HOMEOSTASIS

As sex hormones, both androgens and estrogens play important role in energy homeostasis. More importantly, these two steroid hormones have sex-specific effects. Although the general roles of androgens and estrogens in metabolic syndromes or energy metabolism have been investigated, but the fat tissue specific role of these two hormones are still not clear.

The main function of adipose tissue is to store fat and adipose tissue research focused for many years on biochemical characterization how fat synthesis and breakdown through lipogenesis and lipolysis are regulated (85). In recent research, adipose tissue was demonstrated as the main tissue for sex steroid metabolism (86) and production of adipokines, an endocrine factor that is negatively correlated with obesity in rodents it became clear that adipose tissue is a highly active endocrine organ (87-89). The dysfunction of adipose tissue initiates the development of obesity and other metabolic disorders (87-90). AT dysfunction is characterized by predominantly visceral fat accumulation (86), changes of beneficial adipokines secretion, increased number of AT infiltrating immune cells, enlarged adipocytes, as well as changes in AT mRNA and protein expression patterns (89, 91 and 92).

STS catalyzes the sulfation of steroid sulfates to produce active steroids (estrogens and

androgens), and it tightly regulates the biological homeostasis of the steroid hormones. Previously, our group published the liver specific beneficial role of STS in energy metabolism. Specifically, the beneficial role of STS in obese female mice was through estrogen signaling. In this study, I represented the first attempt to comprehensively dissect the sex- and tissue- specific role of STS in energy homeostasis in AT. Our results showed that overexpression of STS decreased AT derived adiponectin secretion, suppressed adipogenesis, increased fat accumulation and aggravated HFD induced diabetic phenotype in males though increasing AT androgenic activity. While, STS overexpression in female AT presented the opposite phenotypes via increased estrogen signaling. Results from this study may establish STS as a potential therapeutic target to manage metabolic diseases, like type 2 diabetes and obesity.

4.1 METHOD

4.1.1 Generation of STS transgenic mice, diet and drug treatment, body composition analysis, and indirect calorimetry.

The human STS cDNA was cloned into the TRE-SV40 transgene cassette (93) to construct the TRE-STS transgene. Transgenic production was performed at University of Pittsburgh Transgenic Core Facility. The TRE- STS/ aP2-tTA double transgenic which is termed as aP2-STS mice were generated by cross-breeding the TRE-STS mice with the aP2-tTA mice (94) and maintained in the C57BL/6J background. The TRE-STS line expresses STS under the control of the tetracycline response element (TRE). The aP2-tTA line expresses the tetracycline transactivator (tTA) in the adipose tissue. In the double transgenic mice, the tTA protein binds to TRE and initiates the expression of the transgenic STS. Administration of doxycycline (DOX, 2mg/ml) was given in drinking water one week before HFD treatment until the end of experiments. HFD (Cat # S3282) with 60% of total calories coming from animal fat was purchased from Bio-serv (Frenchtown, NJ). Body composition by EchoMRI and indirect calorimetry by Oxymax Indirect Calorimetry System were performed as we have previously described (95). The use of mice in this study has complied with relevant federal guidelines and institutional policies.

4.1.2 Western Blot.

Protein samples will be isolated using RIPA buffer and resolved by electrophoresis on 10% SDS-polyacryl- amide gels. Follow by transferring of proteins to polyvinylidene difluoride (PVDF) membranes; the membranes were probed with primary antibodies against STS (cat#

ab62219) from Abcam (Cambridge, MA). Detection was achieved by using an ECL system from Amersham (Piscataway, NJ).

4.1.3 STS enzymatic activity.

Liver or adipose tissue was minced with scissors in ice-cold 0.25M Tris-HCl buffer, pH 7.5, (1:10 w:v for adipose tissue; 1:20 w/v for liver) and homogenized with a Tissue Tearor (BioSpec) using three 30 sec bursts. Protein concentrations of the homogenates were determined using a Pierce BCA assay (ThermoFisher).3H-estrone sulfate (53 Ci/mmol; Perkin Elmer-NEN) was diluted in 50mM Tris-HCl buffer and 100 µl (140,000 dpm) were added to all assay tubes. Radioinert estrone sulfate (Sigma) was dissolved in ethanol and then diluted into 50mM Tris-HCl buffer and 100 µl was added to achieve a final concentration of 10µM. Experimental compounds were dissolved in ethanol and then diluted in 50mM Tris-HCl buffer. The assay tubes containing steroids were preincubated for 5 min at 37˚ C in a water bath. The assay was initiated by addition of homogenates (300µl) to the tubes. Control samples (background) received 300µl of buffer in place of homogenates. After 30min of incubation at 37˚ C, 3 ml of toluene was added to the tubes. The tubes were vortexed for 1min and centrifuged at 1500xg for 10min. Two 500µl aliquots of the organic phase were removed from each sample and added to 4ml of scintillation cocktail (Ultima Gold, Perkin Elmer) in scintillation vials. Vials were placed in a Packard Tri-Carb scintillation counter for determination of product formation, with 50% efficiency for 3H. Each sample was run in duplicate.

4.1.4 Serum and liver tissue chemistry.

Serum levels of triglycerides (Cat # 2100-430 from Stanbio), cholesterol (Cat # 1010-430 from Stanbio), and insulin (Cat # 90080 from Crystal Chem) were measured using commercial assay kits. The liver concentration of Acetyl-CoA was measured using the PicoProbe Acetyl CoA Assay kit (ab87546) from Abcam (Cambridge, MA).

4.1.5 Gene expression analysis.

RNA was extracted by using the Trizol Reagent (Invitrogen). One microgram of RNA from each sample was reverse transcribed into cDNA using reverse transcriptase (Superscript II, Invitrogen) and oligoDT (Invitrogen). Quantitative RT-PCR was performed with an ABI Prism 7000 Thermal Cycler (Applied Biosystems) using SYBR Green detection reagent. GAPDH was used as the housekeeping control gene. Relative gene expression was calculated using the ΔΔCT method, where fold difference was calculated using the expression $2^{-\Delta\Delta Ct}$.

4.1.6 Glucose tolerance test (GTT) and insulin tolerance test (ITT).

For GTT, mice received an intraperitoneal injection of D-glucose at 2 g/kg body weight after a 12-h fasting. For ITT, mice received an intraperitoneal injection of insulin at 0.5 units/kg body weight after a 6-h fasting.

4.1.7 Histology Study.

Tissues were fixed in 4% formaldehyde, embedded in paraffin, sectioned at 5 μm, and stained with hematoxylin-eosin (H-E) (19). For immunofluorescence, tissue sections were deparaffinized and rehydrated, followed by preincubated in blocking buffer (13 PBS, 5% normal donkey serum, and 0.3% Triton X-100) for 60 min. Tissue sections were then incubated with diluted primary antibody overnight at 4°C and fluorochrome-conjugated secondary antibody for 1 to 2 h at room temperature in dark the next day. Antibodies used include goat anti-mouse CD68 (M-20) polyclonal antibody (catalog number sc-7084; Santa Cruz Biotechnology). Histomorphometric analysis on insulin-stained pancreatic sections was per- formed using ImageJ from the National Institutes of Health (Bethesda, MD), and the percent of islet area per total pancreatic area was calculated (20). b-cell mass was determined by multiplying the percentage of islet area per pancreatic area by the pancreatic weight. Pancreatic b-cell proliferation and apoptosis were determined on insulin-stained pancreatic sections by Ki67 immunostaining (Ki67 antibody clone SP6; Neomarkers) and terminal deoxy-nucleotidyl transferase-mediated dUTP nick end-labeling (TUNEL) assay from Promega (Madison, WI), respectively.

4.1.8 UPLC-MS/MS analysis of adipose tissue estrogens and estrogen sulfates.

UPLC/MS-MS were carried out with a Waters Acquity UPLC system connected with the Xevo TQ triple quadrupole mass spectrometer as we have previously described (96).

4.1.9 Statistical analysis.

Data are expressed as the means ± standard deviations (SD). One-way analysis of variance (ANOVA) Tukey's test was performed for statistical analysis using GraphPad Prism (San Diego, CA). P values of less than 0.05 were considered statistically significant.

4.1.10 Study approval.

The Central Animal Facility of the University of Pittsburgh is fully accredited by the American Association for Laboratory Animal Care (AALAC). All procedures were performed in accordance with relevant federal guidelines and with the approval of the University of Pittsburgh ethical committee.

4.2 RESULTS

4.2.1 The adipose expression of STS was induced in obese mice, and the creation of transgenic mice expressing STS in adipose tissue.

High-fat diet (HFD) feeing is commonly used mouse model of obesity and type 2diabetes.We found the expression of endogenous Sts was induced in the epididymal white adipose tissue (epi-WAT) of after challenging mice with HFD (Fig. 9A), indicating the possibility of sex-specific role of STS in AT energy homeostasis. To understand the functional relevance of STS induction and to determine the metabolic effect of STS in vivo, we generated tetracycline-inducible STS transgenic (Tg) mice expression human STS in the adipose tissue (Fig. 9B). The Tet-off transgenic system was composed of two transgenic lines with one line (TetRE-STS) expressing hemagglutinin (HA)-tagged STS (HA-STS) under the control of a minimal cytomegalovirus promoter (pCMV) fused to the tetracycline-responsive element (TetRE), and the other line (aP2-tTA) expressing the tetracycline-transcriptional activator (tTA) in the adipose tissue under the control of the aP2 gene promoter. In mice carrying both transgenes (aP2-STS), tTA would bind to TetRE and induce the expression of STS, whereas treatment with doxycycline (DOX) would dissociate tTA from TetRE and thus silence the expression of STS. The expression of the transgenic STS and its silencing by DOX in the adipose tissue tissue was confirmed by RT-PCR and Western blotting (Fig. 9C). The transgene was undeteactable in non-targeting tissues, including the liver and skeletal muscle (data not shown). The adipose expression of the transgene was also confirmed at the enzymatic level by using the tritium-labeled estrone sulfate as substrate (Fig. 9D). It was noted that the adipose expression of the transgene was comparable between the male and female Tg mice (Fig. 9E).

Bi et al., Fig. 9

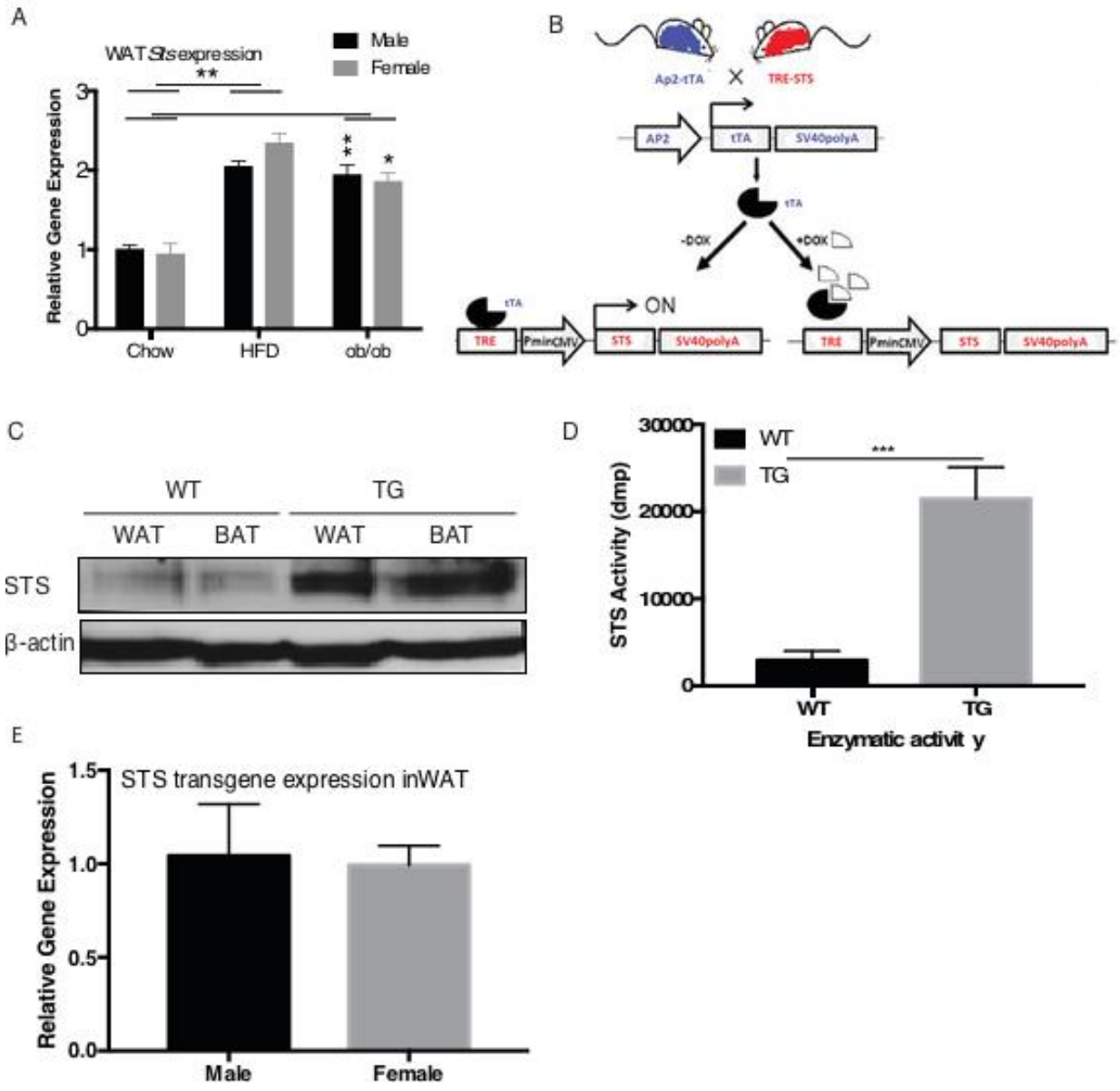

Figure 9 The AT expression of STS was induced in obese mice, and creation of transgenic mice expressing STS in AT.

(A) The mRNA expression of mouse *Sts* in the epididymal white adipose tissue (Epi-WAT) of chow-fed Wt mice, high-fat diet (HFD)-fed wild-type (Wt) mice, and chow-fed ob/ob

mice. **(B)** The schematic representation of the Tet-off STS transgenic system. aP2, fatty acid binding protein 4; tTA, tetracycline transcriptional activator; SV40 polyA, simian virus 40 polyadenylation signal; TRE, tetracycline response element; Pmin, minimal human cytomegalovirus promoter. **(C)** The expression of STS protein in the WAT and brown adipose tissue (BAT) of the Wt and transgenic (Tg) mice was measured by Western blotting. **(D)** The adipose STS enzymatic activity was determined by estrone sulfate conversion assay and was normalized against protein concentrations. **(E)** The adipose expression of the STS transgene in female and male Tg mice was measured by real-time PCR. n=4 mice per group. * or #, $P<0.05$; ** or ##, $P<0.01$; ***, $P<0.001$, compared to Chow of the sex (A), or compared to the Wt (D).

4.2.2 AT over-expression of STS aggravated HFD-induced adiposity, insulin resistance, and glucose intolerance in male mice.

When challenged with HFD for 20 weeks, male, but not female, aP2-STS Tg (AS) male mice showed significant increase in body weight compared with age-matched WT littermates (Fig. 10A). Body composition analysis by magnetic resonance imaging revealed that the gain of body weight in AS males was largely accounted for by the increase of fat mass, while lean mass was not affected (Fig. 10A). Specifically, it was the mass of epi-WAT of AS male but no other AT showed significant increase (Fig. 10B). The body weight gain was achieved without significant changes in food intake (Fig. 10C). Visceral adipose tissue (mainly epi-WAT) mass correlates with development of insulin resistance, while total or subcutaneous adipose tissue mass does not (98). It has been thoroughly confirmed that the adipocytes of visceral fat tissue are more lipolytically active than subcutaneous adipocytes and thus contribute more to the plasma free fatty acid levels (97). This is also consistent with the phenotype observed in HFD challenged AS mice, thus in our study we mainly focused on epi-WAT. Metabolic cage analysis showed the oxygen consumption and energy expenditure was significantly decreased in HFD-fed AS males (Fig. 10D). When the whole-body insulin sensitivity was evaluated, we found that the AS males showed fasting

hyperglycemia and worse performance in Glucose Tolerance Test (GTT) and Insulin Tolerance Test (ITT) (Fig. 10E and F). To directly assess the insulin sensitivity in AT, we harvested and assessed AT tissues for the phosphorylation of Akt (protein kinase B) by Western blotting. Decreased Akt phosphorylation was observed in WAT, but not in the liver and skeletal muscle, suggesting a WAT-specific of insulin resistance (Fig. 10G). Histological analysis of pancreatic sections showed no difference in islet size and total islet area, in HFD challenged AS males and WT littermates. This could suggest it was not the alterations in b-cell proliferation and/or death in AS males that worsened the whole-body insulin resistance (Fig. 10K). The AS males also showed increased serum level of triglycerides, decreased serum level of free fatty acid, but the serum cholesterol level was not affected (Fig. 10 I, J and K).

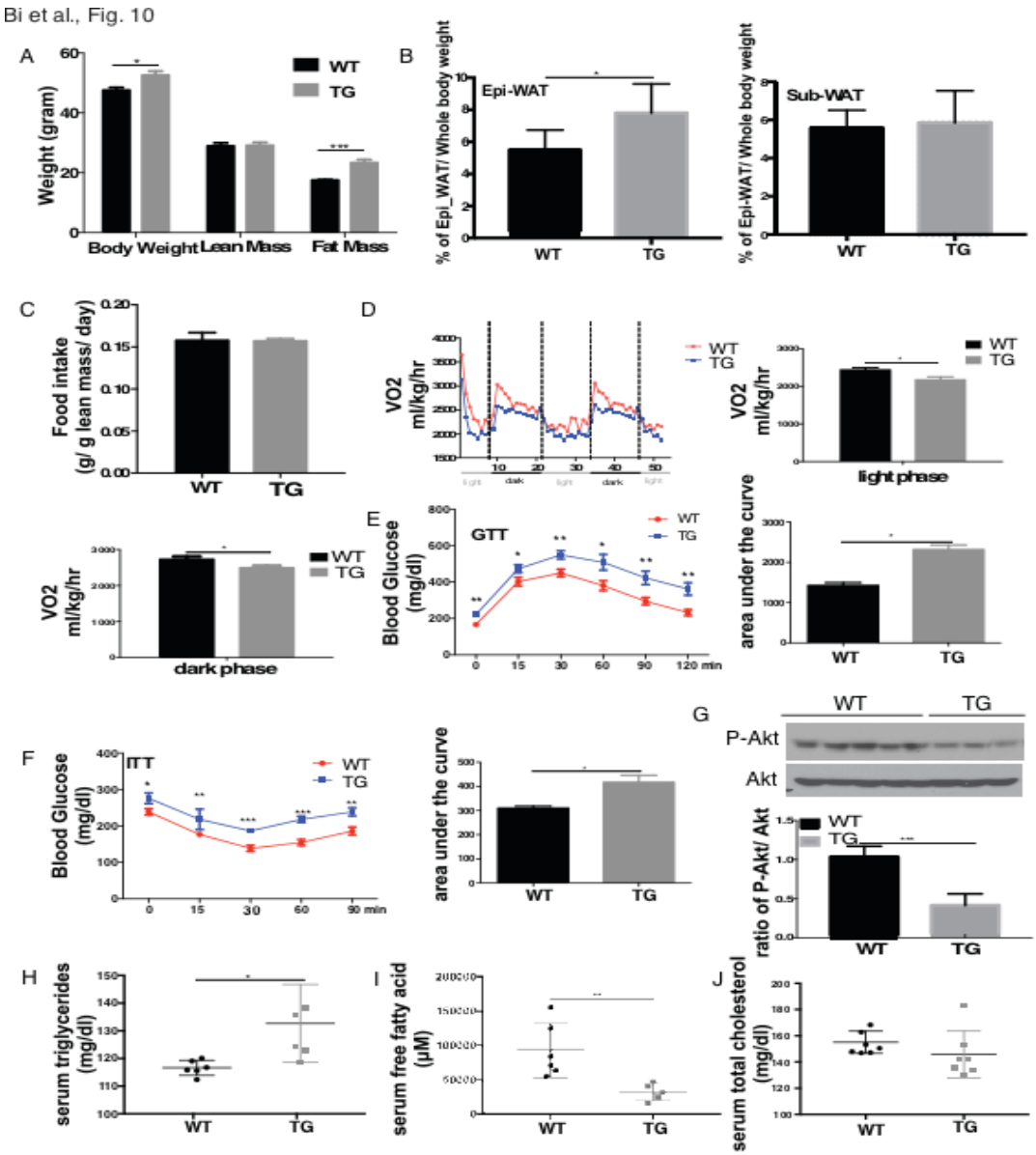

Figure 10 AT over-expression of STS aggravated HFD-induced adiposity, insulin resistance, and glucose intolerance in male mice.

All mice are males. Mice were fed with HFD for 20 weeks before analysis. **(A-F)** Mice were analyzed for body weight and body composition (A), fat mass (B), food intake (C), oxygen consumption (D), GTT (E) and ITT (F). The quantifications of the GTT and ITT results are shown as the areas under the curve. **(G)** Western blot analysis of Akt phosphorylation in epi-WAT. Shown below is the densitometric quantification of the Western blotting results. **(H-J)** The serum levels

of triglycerides (H), free fatty acids (I), and total cholesterol (J). Results are expressed as mean ± SD. n=4 mice per group. *, $P<0.05$; **, $P<0.01$, compared to the Wt.

4.2.3 AT over-expression of STS decreased adipogenesis and lipolysis and aggravated HFD- induced adipose and systemic inflammation in males.

When the gene expression in epi-WAT was profiled, the Tg male showed a decreased expression of two key lipolytic lipases, hormone sensitive lipase (Hsl) and adipose triglyceride lipase (Atgl) (Fig. 11A). The epi-WAT expression of Lipoprotein lipase (LPL) was also reduced in Tg male mice, an enzyme that hydrolyses meal-derived triglycerides in chylomicrons and very low-density lipoprotein triglyceride at the capillary endothelium, which regulates the major path way of free fatty acid uptake (99) (Fig. 11C). This was consistent with the increased epi-WAT fat mass and reduced level of serum free fatty acids (Fig.10B and Fig. 10I). Additionally, the expression of the glucose uptake transporter Glut4 and uncoupling protein 1 (UCP1) responsible for energy expenditure was downregulated in the epi-WAT of the Tg males (Fig. 11B). There were no changes in the expression of lipogenic genes, but the expression adipogenic genes or genes indicative of adipogenesis was significantly decreased in the epi-WAT of Tg males (Fig. 11C). The down-regulation of peroxisome proliferator activated receptor γ (PPARγ) and phosphorylated Erk was confirmed by Western blotting (Fig. 11D). PPARγ is a master regulator of adipogenesis (100, 101), whereas the activation of Erk1/2 is required for the cell proliferation in the early phase of adipogenesis. Consistent with the inhibition of adipogenesis (102,103). We then went on to test the adipocyte secreted adipokine levels. The epi-WAT expression of the beneficial adipokine

adiponectin was decreased in the Tg males (Fig. 11E), which may have contributed to the worse metabolic function in Tg males.

Obesity is commonly associated with chronic and low-grade inflammation primarily originated from the excess of adipose tissue, which often leads to elevated circulating levels of proinflammatory cytokines such as Il-6 and Tnfα (103). We then analyzed the epi-WAT local and systemic inflammation to determine whether the transgene aggravated fat tissue inflammation and contributed to obesity-associated insulin resistance in the males. Immunostaining of Cd68, a macrophage marker gene, showed that the epi-WAT of Tg males had a substantially increased number and size of the crown-like structures compared with the Wt males (Fig. 11F). Both the serum level of Il-6 (Fig. 11G) and adipose expression of pro-inflammatory marker genes (Fig. 11H) were elevated in Tg males. The average size of adipocytes in the epi-WAT of the Tg males was larger than that of the Wt mice (Fig. 11I). It is known that the increase of cytokine level with diet induced obesity positively correlates with adipocyte size (103). The adipose hypertrophy may contribute to the bigger Ep1-WAT fat pad and decreased lipolysis (Fig. 10A and 10B).

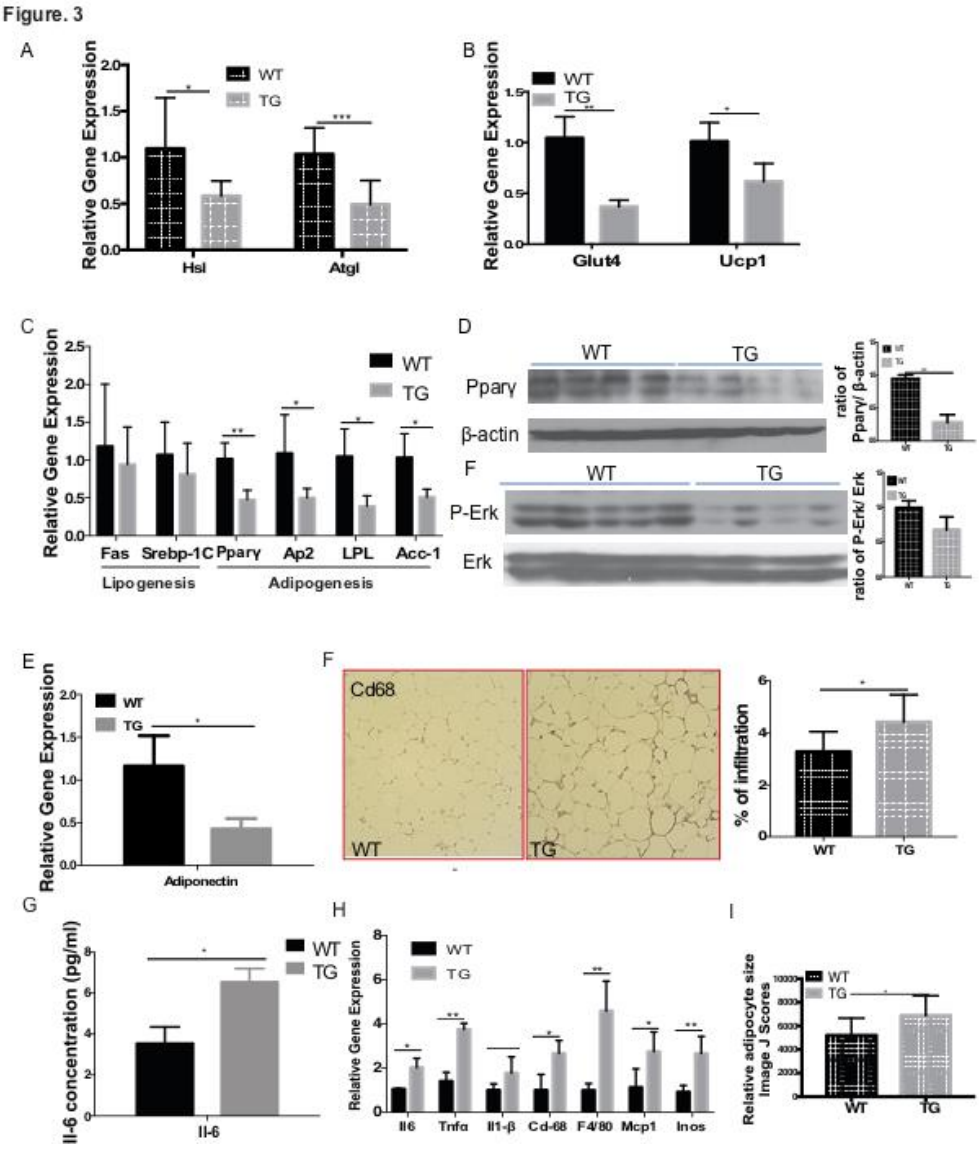

Figure 11 AT over-expression of STS decreased adipogenesis and lipolysis and aggravated HFD- induced adipose and systemic inflammation in males.

Mice are the same as described in Fig. 10. **(A-C)** The epi-WAT expression of genes responsible for lipolysis (A), glucose uptake and energy expenditure (B), lipogenesis and adipogenesis (C) was measured by real-time PCR. **(D)** The protein level of PPARγ and ERK1/2 was measured by Western blotting. **(E)** The The epi-WAT expression of adiponectin. **(F)** Immunostaining of Cd68. Shown on the right is the quantification. **(G and H)** The serum level of IL-6 (G) and adipose expression on pro-inflammatory genes and macrophage marker genes (H). Results are expressed as mean ± SD. n=4 mice per group. *, $P< 0.05$; **, $P<0.01$; ***, $P<0.005$, compared to the Wt.

4.2.4 The adverse effects of STS AT overexpression in male mice were mediated through androgen pathway.

Since the primary function of STS is to de-sulfonate and re-activate estrogens and androgens, and estrogens and androgens are known to regulate the metabolic functions of in rodents and humans (1, 2), we went on to determine whether the aggravation of metabolic function in the Tg males was due to increased estrogenic or androgenic activity in the adipose tissue. In HFD-fed, adipose expression of a panel of estrogen responsive genes was not different between the Wt and Tg males (Fig. 12A), which was consistent with the unchanged adipose concentrations of estrone and estradiol in the Tg males (Fig. 12B). When the androgen activity in the epi-WAT was measured, we found the expression of genes that are positively regulated by androgens, such as Eefia2 and Mylk (104), were increased in Tg males, whereas the expression of genes known to be suppressed by androgens, such as Cebpd, Apoc2 and Mtl (60), were significantly decreased in Tg males (Fig. 12C). Consistent with the pattern of gene regulation, the tissue level of testosterone in the epi-WAT, but not the liver, was elevated in the Tg males (Fig. 12D), but the circulating level of testosterone was not affected (Fig. 12E). The gene regulation was adipose specific, because the expression of androgen responsive genes was not affected in the liver and skeletal muscle of the Tg males (Fig. L and M).

To further evaluate whether the transgenic phenotype was androgen dependent, we performed castration on 4-week-old males to remove the primary source of androgen. The castrated mice were then challenged with HFD for 20 weeks. Castration had little effect on the expression of the transgene (data not shown), but it abolished the transgenic phenotypes in body weight gain and fat mass gain (Fig. 12F), oxygen consumption (Fig. 12G), GTT and ITT (Fig.

12H), adipose inflammation at the histological (Fig. 12I) and inflammatory gene expression (Fig. 4J) levels. The regulation of androgen responsive genes was normalized upon castration as expected (Fig. 12K). These results suggested that the adverse metabolic effects in male STS mice were estrogen- dependent.

Bi et al., Fig. 12

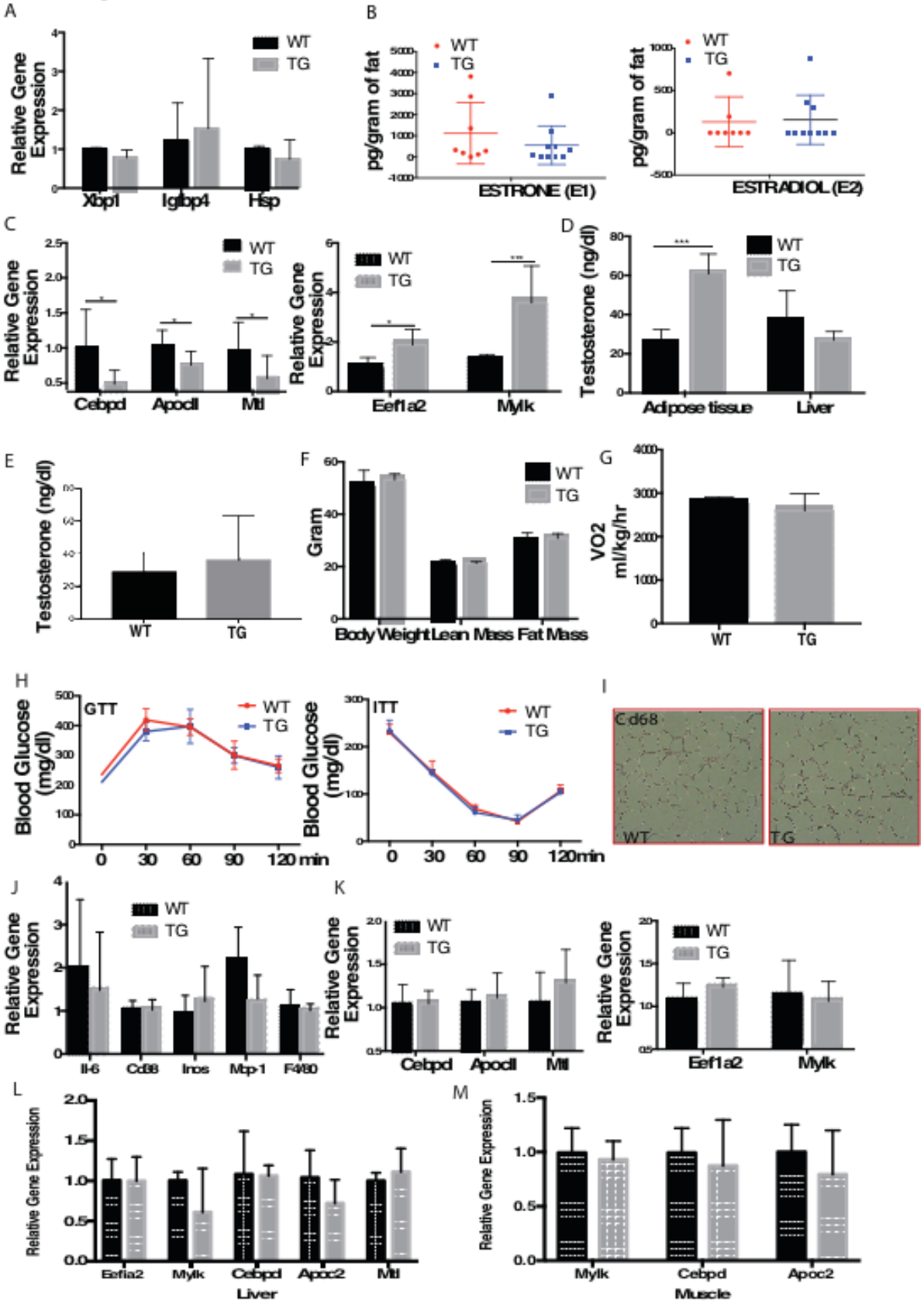

Figure 12 The effects of STS AT overexpression in male mice were mediated through androgen pathway.

(A-E) Mice are the same as described in Fig. 2. Shown are adipose expression of estrogen responsive genes (A) adipose levels of estrogens (B), adipose expression of androgen responsive genes (C), adipose and liver levels of testosterone (D), the serum levels of testosterone (E). **(F-M)** Male mice were castrated before being fed with HFD for 20 weeks. Shown are body weight and body composition (F), oxygen consumption (G), GTT and ITT (H), immunostaining of CD68 (I), adipose expression of pro-inflammatory genes and macrophage marker genes (J), and adipose expression of androgen responsive genes (K). (L and M), Shown are the expression of androgen responsive genes in the liver (A) and skeletal muscle (B). Results are expressed as mean ± SD. n=4 mice per group. *, $P< 0.05$; **, $P<0.01$; ***, $P<0.005$, compared to the Wt

4.2.5 AT over-expression of STS ameliorated HFD- induced obesity, insulin resistance, glucose tolerance and inflammation in female mice.

Interestingly, the adipose STS transgenic effect was sex specific, because the phenotypes in Tg females were totally opposite to those observed in Tg males. Specifically, the Tg females showed a reduced body weight gain, which was due to reduced fat mass (Fig. 13A). The mass of perigonidal adipose tissue (peri-WAT), but not the subcutaneous WAT, was decreased in Tg females (Fig. 13B). The food intake was not affected by the transgene (Fig. 13C). The oxygen consumption in the dark phase was significantly increased (Fig. 13D). The Tg females also showed a significantly lower fasting glucose level and better performance in GTT (Fig. 13E) and ITT (Fig. 13F). The peri-WAT levels of phosphorylated Irs-1 and Akt were increased in the Tg females (Fig. 13G), further suggesting an improved insulin sensitivity. Histological analysis of the pancreas showed no difference in total islet area and islet size (Fig. 13H). The Tg females also showed a reduced serum level of triglycerides (Fig. 13H), but no change in the serum cholesterol (Fig. 13I).

Opposite to that of male Tg mice, the serum free fatty acid level was increased in female Tg mice (Fig. 13J).

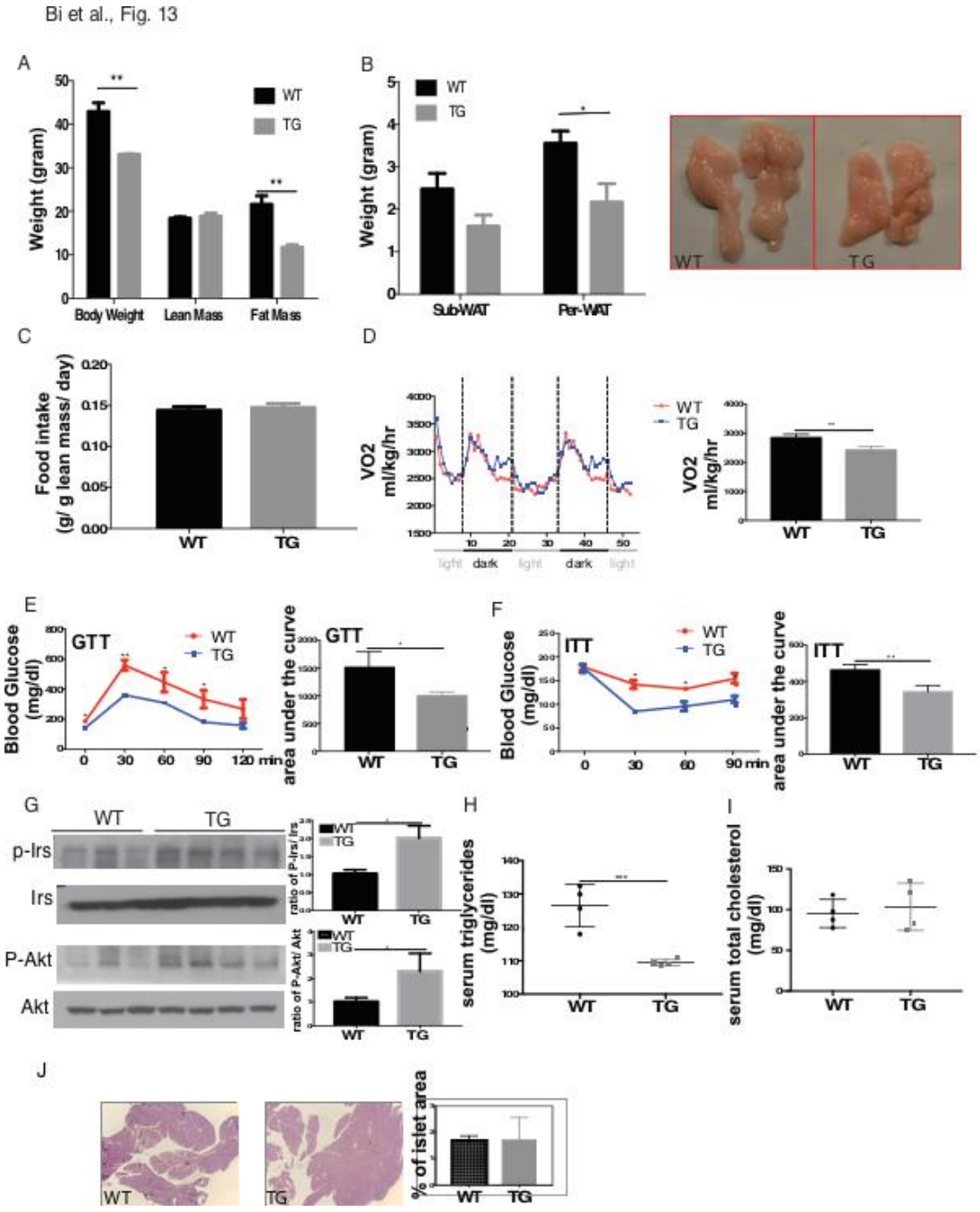

Figure 13 AT Over-expression of STS alleviated HFD-induced obesity and improved insulin sensitivity.

All mice are females. Mice were fed with HFD for 20 weeks before analysis. **(A-F)** Mice were analyzed for body weight and body composition (A), fat mass (B), food intake (C), oxygen consumption (D), GTT (E) and ITT (F). The quantifications of the GTT and ITT results are shown as the areas under the curve. **(G)** Western blot analysis of Irs-1 and Akt phosphorylation in epi-WAT. Shown on the right are the densitometric quantifications of the Western blotting results. **(H and I)** The serum levels of triglycerides (H) and total cholesterol (I). (J) Shown are H&E staining of pancreatic sections and the Image J quantifications of pancreatic islets areas. Results are expressed as mean ± SD. n=4 mice per group. *, $P<0.05$; **, $P<0.01$, compared to the Wt.

4.2.6 AT over-expression of STS increased energy uptake, AT adipogenesis and ameliorated HFD- induced adiposity and systemic inflammation in females.

Tg females showed increased expression of glucose uptake transporter Glut4 and uncoupling proteins in the peri-WAT (Fig. 14A). The expression of adipogenic genes was increased in the peri-WAT of Tg females (Fig. 14B), opposite to the suppression in the Tg males. The induction of PPARγ was confirmed at the protein level by Western blotting (Fig. 14C). Both the peri-WAT expression (Fig. 14D) and circulating level of adiponectin (Fig. 14E) were elevated in the Tg females. Consistent with improved metabolic functions and insulin resistance, Tg females showed attenuated HFD-induced adipose and systemic inflammation, as evidenced by decreased crow-like structures (Fig. 14F), decreased expression of pro-inflammatory genes (Fig. 14G), and a decreased circulating level of Il-6 (Fig. 14H).

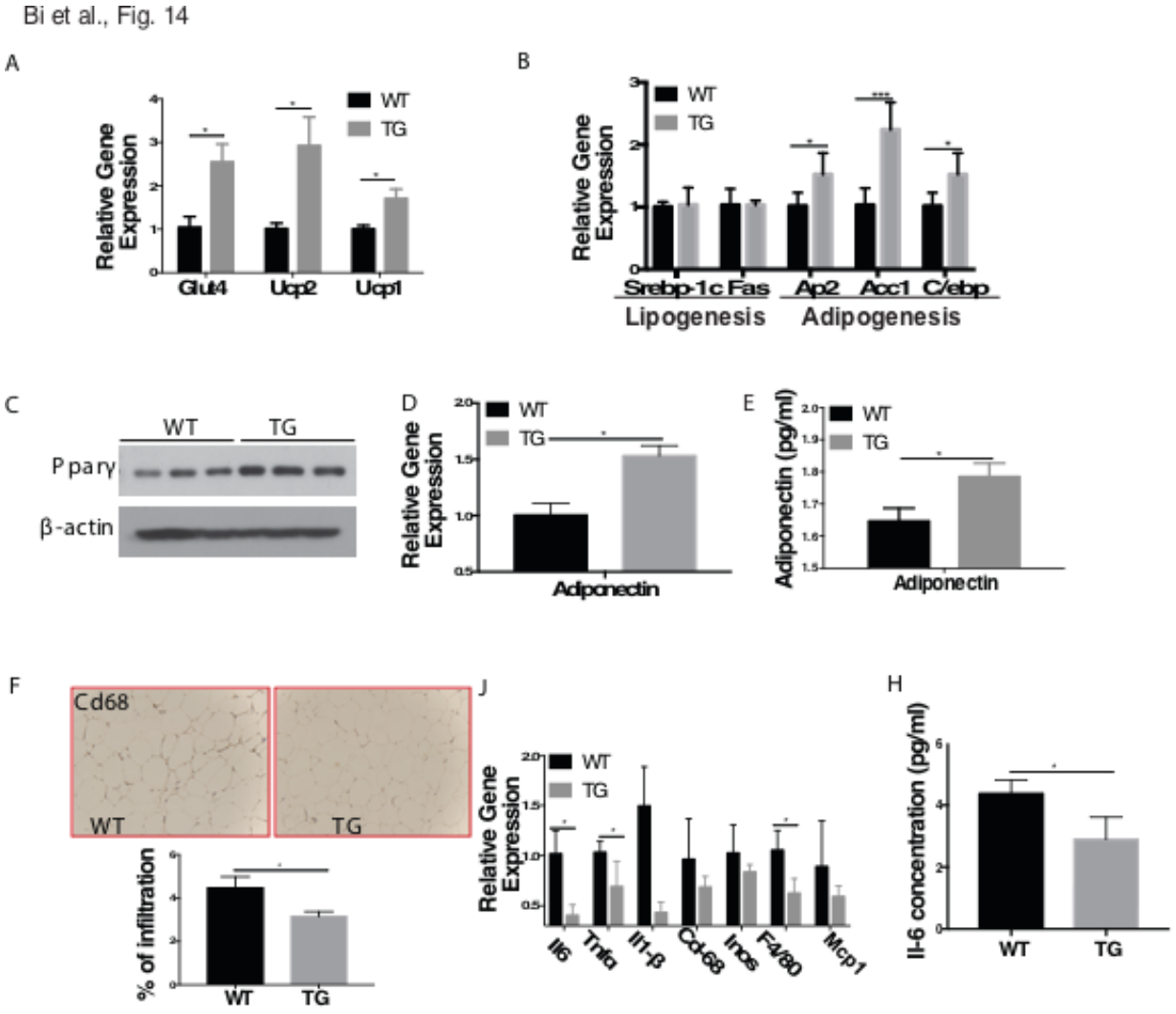

Figure 14 AT over-expression of STS increased energy uptake, AT adipogenesis and ameliorated HFD- induced adipose and systemic inflammation in females.

Mice are the same as described in Fig. 13. **(A and B)** Adipose expression of genes responsible for energy uptake and expenditure (A), and lipogenesis and adipogenesis (B) was measured by real-time PCR. **(C)** The protein level of PPARγ was measured by Western blotting. **(D and E)** The adipose mRNA expression of adiponectin (D) and the serum level of adiponectin (E). **(F)** Immunostaining of Cd68. Shown below is the quantification. **(G and H)** Adipose expression of pro-inflammatory genes and macrophage marker genes (G), and the serum level of Il-6 (H). Results are expressed as mean ± SD. n=4 mice per group. *, $P<0.05$; **, $P<0.01$, compared to the Wt.

4.2.7 The metabolic benefit of female AS mice was estrogen-dependent.

In understanding the metabolic benefit in the Tg females, we found the expression of estrogen responsive genes (Fig. 15A), but not the androgen responsive gene (Fig. 15B), was induced in the peri-WAT. To further determine whether the metabolic benefit was estrogen dependent, we eliminated the primary source of endogenous estrogens from 4-week-old pre-pubertal female mice by ovariectomy before challenging them with HFD for 20 weeks. Upon overiectomy, the expression of estrogen responsive genes in the per-WAT of Tg females no longer showed changes (Fig. 15C), whereas the expression of the STS transgene was not affected (data not shown). Ovariectomy completely abolished the metabolic benefit of the STS transgene in body weight and body composition (Fig. 15D), oxygen consumption (Fig. 15E), GTT and ITT (Fig. 15F), adipose inflammation at the histological (Fig. 15G) and inflammatory gene expression levels (Fig. 15H), and the expression of adipogenic genes (Fig. 15I). Taken together, these data showed that the STS effects in female adipose tissue is mediated through estrogen signaling pathway.

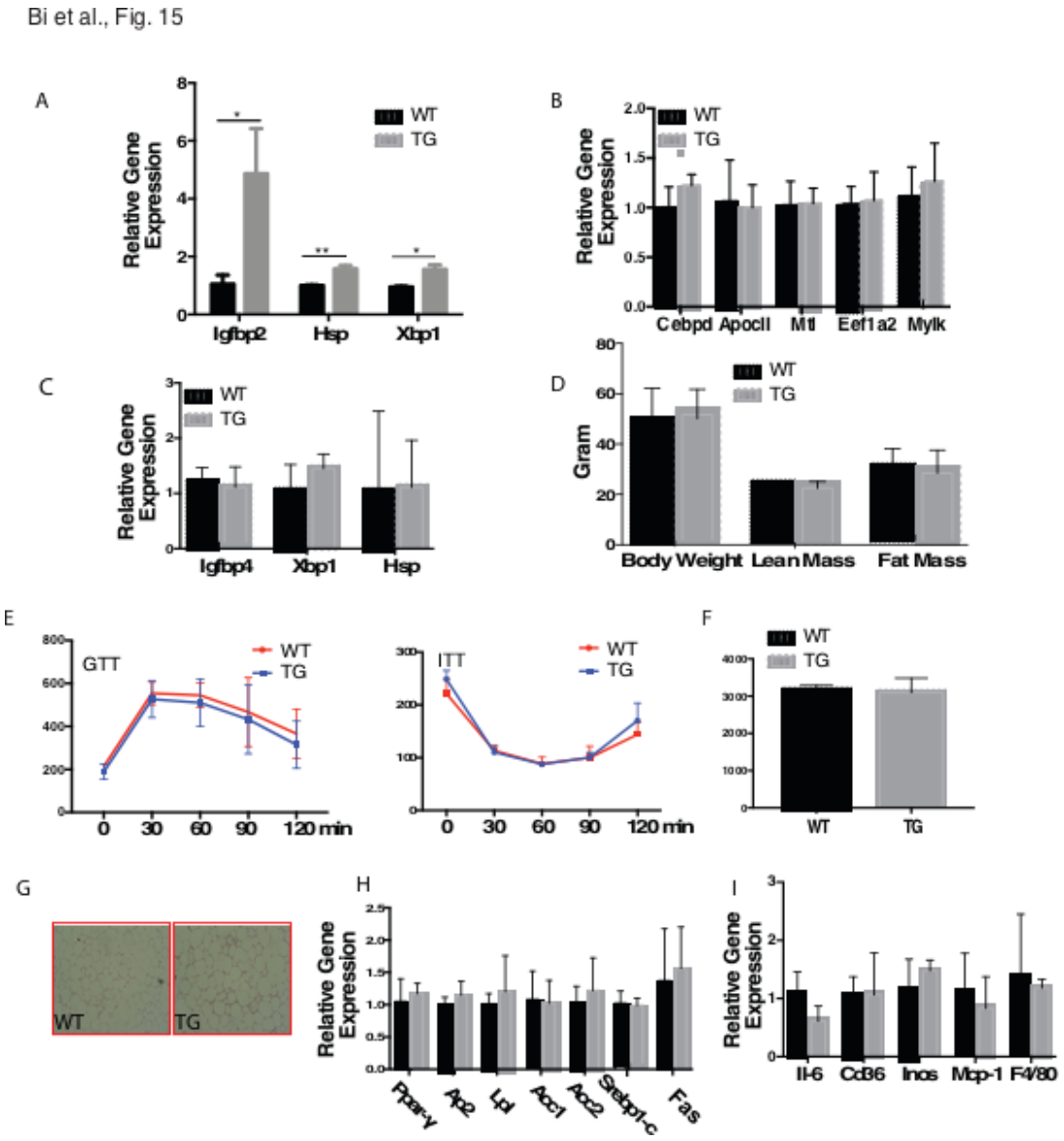

Figure 15 The effects of STS AT overexpression in female mice were mediated through estrogen pathway.

(A and B) Mice are the same as described in Fig. 5. Shown are adipose expression of estrogen responsive genes (A) and androgen responsive genes (B) as measured by real-time PCR. **(C to I)** Female mice were ovariectomized before being fed with HFD for 20 weeks. Shown are adipose expression of estrogen responsive genes (C), body weight and body composition analysis (D), oxygen consumption (E), GTT and ITT (F), immunostaining of CD68 (G), adipose expression of pro-inflammatory genes and macrophage marker genes (H), and genes involved in adipogenesis and lipogenesis (I). Results are expressed as mean ± SD. n=4 mice per group. *, $P<0.05$; **, $P<0.01$, compared to the Wt.

4.3 DISCUSSION

In this study, we reported the adipose induction of Sts in mouse models of obesity and insulin resistance. Based on our results, the adipose induction of Sts in response to metabolic stress appears to have a sex-specific outcome: it may represent a protective response in females because of increased estrogen activity in the adipose tissue; whereas in males, the induction may have exacerbated the metabolic harm in an androgen- and inflammation-dependent manner. Under the control of the aP2 gene promoter, the STS transgene had the most obvious effect in epi-WAT, whereas the subcutaneous WAT and brown adipose tissue showed little appreciable microscopic and functional phenotypes although the transgene was efficiently expressed in these two fat depots (data not shown). The fat depot specific effect of the STS transgene remains to be understood.

One of the most interesting observations is the sex-dimorphic effect of STS in the adipose tissue. Sex dimorphisms have been documented in many aspects of the metabolic syndrome, ranging from fat distribution to sex hormone levels. We found that overexpression of STS in the adipose tissue of male mice aggravated HFD-induced obesity, insulin resistance and inflammation. The worsened metabolic functions in the Tg males were likely resulted from induced androgen reactivation and increased androgenic activity in the adipose tissue, whereas castration abolished these adverse effects. These results underscored the importance of adipose androgen signaling in energy homeostasis. It has been suggested that aromatization of testosterone into estrogens is critical to energy homeostasis in males. However, our results showed the STS transgene had little effect on the adipose expression of estrogen responsive genes and adipose tissue levels of estrogens in Tg males, indicating that the phenotype was specifically caused by increased androgen signaling. The HFD-fed Tg females, on the other hand, exhibited improved metabolic functions

that included the relief of insulin resistance and adipose inflammation. The metabolic benefit of STS in female mice was estrogen dependent, because the responsive genes of estrogens but not androgens were induced in the adipose tissue. Moreover, overiectamy abolished the metabolic benefit of the STS transgene, further suggesting that estrogens have mediated the metabolic benefit in Tg females.

Another interesting finding is the sex hormone dependence of the phenotype. The primary function of the STS enzyme is to convert androgen sulfates and estrogen sulfates to hormonally active androgens and estrogens. By prediction, the androgen and estrogen levels should be increased in the adipose tissue of the Tg mice. Our previously work has largely focused on the the role of STS in estrogen conversion. For example, liver-specific transgenic expression of STS enhanced estrogen activity and conferred the metabolic benefits in female Tg mice (72). In human livers and human liver cells, chronic inflammation activates NF-κB and induces the expression of STS, which was reasoned to be a major contributor for the estrogen excess in male patients of chronic inflammatory liver diseases (105). To our knowledge, the current work represents the first study focusing on the role of STS in androgen conversion. Generally, androgens are believed to play opposite roles in energy homeostasis in males and females. It has been reported that deficiency of androgen worsens metabolic functions in males, while androgen excess worsens metabolic functions in females (1). In males, the impact of testosterone deficiency on the development of visceral obesity, insulin resistance and metabolic syndrome in men has also been reported (28-30). Androgens are known to confer metabolic benefits in many tissues in males, including the liver, pancreatic β-cells, and skeletal muscle. For adipose tissue, there is an inverse correlation between total serum testosterone and the amount of visceral adipose tissue (48). On one hand, this could be

explained by the coverstion of androgens into estrogens by aromatase to provide estrogens for tissue metabolism. Indeed, orchidectomized male rodents treated with either testosterone or estrogen remain lean, while those treated with the pure androgen DHT that cannot be converted to esteogen develop obesity (106). This is also true in men for whom testosterone replacement suppresses adiposity, and this effect is blocked in the presence of an aromatase inhibitor (107). On the other hand, most of the reported effects of androgens on adipose tissue in males were believed to be indirectly mediated by AR signaling in the skeletal muscle (42-44). One of a few studies focusing on the specific role of androgens in adipose tissue is using adipocyte-specific androgen receptor knockout mice, in which these mice showed no difference in subcutaneous and epididymal fat mass in either chow fed condition or HFD condition (48). Furthermore, AR regulates adiponectin production. The serum adiponectin levels are high in hypogonadal men and are reduced by testosterone therapy (108). Testosterone infusion also decreases the level of adiponectin (109), an adipokine that enhances insulin sensitivity (110), reduces chronic inflammation and maintains healthy adipose tissue expansion while rescuing ectopic lipid accumulation in animal models (111). Consistent with the above finding, the adipose expression of adiponectin and the circulating level of adiponectin were decreased in the Tg males, which may have contributed to the metabolic harm of the transgene in this sex. Androgens are known for their anti-adipogenic activity (112), which may have helped to explain the decreased expression of adipogenic genes in the adipose tissue of the Tg males. Taken together, our results have demonstrated direct effects of STS and androgens on the adipose tissue of males.

It is also interesting to note that the sex-dimorphic effect of STS is also tissue specific. We have previously reported that overexpression of STS in the liver of transgenic mice alleviated HFD and

ob/ob models of obesity and type 2 diabetes in both sexes (62). Interestingly, although the metabolic benefits of hepatic STS was conserved in both sexes, it appeared that STS exerted its metabolic benefit through sex-specific mechanisms. In female mice, STS may have increased hepatic estrogen activity by converting estrogen sulfates to active estrogens and consequently improved the metabolic functions; whereas ovariectomy abolished this protective effect. In contrast, the metabolic benefit of hepatic STS in males may have been accounted for by the male-specific decrease of inflammation in white adipose tissue and skeletal muscle, as well as a pattern of skeletal muscle gene expression that favors energy expenditure. The metabolic benefit of the hepatic STS in male mice was intact upon castration. A few notable differences between the adipose STS and hepatic STS Tg mice include: 1) The adipose STS was protective in females but sensitized males to metabolic stress, whereas the hepatic STS was protective in both sexes; 2) Within the male sex, the sensitizing effect of adipose STS was androgen dependent, whereas the protective effect hepatic STS remains to be defined, because the protective effect was intact upon castration; and 3) Also within the male sex, the adipose STS exacerbated adipose inflammation, whereas the hepatic STS attenuated adipose inflammation.

Interesting, the metabolic effect of the estrogen sulfotransferase (EST) is also tissue- and sex-specific. EST sulfonates estrogens and convert them to hormonally inactive estrogen sulfates. We have previously reported that the induction of hepatic *Est* is a common feature of several mouse models of type 2 diabetes. Loss of *Est* in female mice improved metabolic function in *ob/ob* mice as a result of decreased estrogen deprivation and increased estrogenic activity in the liver. Interestingly, the effect of *Est* ablation was sex-specific, as *Est* ablation in *ob/ob* males exacerbated the diabetic phenotype, which was accounted for by increased inflammation in the white adipose

tissue, as well as decreased islet β cell mass and failure of glucose-stimulated insulin secretion (113). Interestingly, although the diabetes induction of *Est* was liver specific, transgenic reconstitution of EST in the adipose tissue, but not in the liver, attenuated diabetic phenotype in male ob/ob mice deficient of *Est* (114). The metabolic benefit of adipose reconstitution of *Est* was sex-specific, because adipose reconstitution of *Est* in female ob/ob mice deficient of *Est* had little effect (114).

In summary, this study uncovered a sex-dimorphic and sex hormone-dependent role of STS in adipose inflammation and energy homeostasis. The adipose STS may represent a novel therapeutic target for the management of obesity and type 2 diabetes.

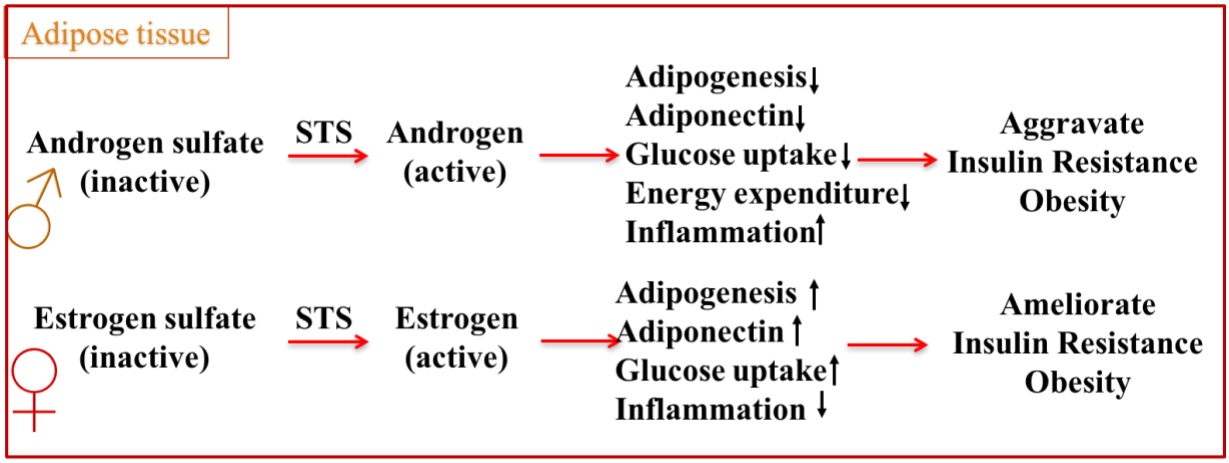

Picture 3 Overview of sex- and adipose tissue specific roles of STS in WAT energy homeostasis.

5.0 **CHAPTER V: SUMMARY AND PERSPECTIVE**

In summary, my thesis points out the importance of sulfotransferase and sulfatase in energy homeostasis. Sult2B1b, as cholesterol sulfotansferase inhibits HNF4α mediated gluconeogenesis. It also confers an endogenous mechanism with HNF4α to inhibit gluconeogenesis. Blood glucose level is mainly regulated by the glucose uptake by the peripheral tissues and the glucose production mostly by the liver (10). Gluconeogenesis is the most essential component to contribute to hepatic glucose production. Therefore, regulating hepatic gluconeogenesis is very essential to regulate whole body blood glucose level (10). Especially, in diabetic condition, increased fasting blood glucose level is mostly led by uncontrolled hepatic gluconeogenesis. We found that in fasting stage, the expression level of both Sult2B1b and HNF4α was induced, and SultB1b$^{-/-}$ mice showed higher fasting blood glucose level. This highly suggests that ablation of Sult2B1b breaking the negative feedback regulation between HNF4α and Sult2B1b would increase blood glucose production and lead to fasting hyperglycemia. On the other hand, this indicates the importance of the restrictive effect of the regulation between HNF4α and Sult2B1b, particularly in diabetic stage.

Our study also demonstrated that Sult2B1b enzymatic product CS and its chemical derivative Thiocholesterol could be important component in this negative feedback regulation to inhibit gluconeogenesis. The level of CS in the feces of SultB1b$^{-/-}$ mice did decrease associated with an increased fasting blood glucose level (data not shown). Thiocholesterol and CS also showed significant inhibitive role in hepatic glucose production in primary hepatocytes. When treat obese mice with these two chemicals, both of them contents high effectiveness in improving whole body glucose homeostasis, insulin resistance and liver steatosis. Moreover, thiocholestol as

a synthesized chemical is hydrolysis resistant and more potential to decrease hepatic blood production and improve the diabetic phenotypes. Considering the potential of thiochloesterol as a therapeutic drug to manage diabetes and obesity, further preclinical study will be followed.

In addition to the liver, HNF4α and SULT2B1b is also expressed in other tissues for example pancreas and adrenal gland (5, 6). Further study will focus on the effect of HNF4α and Sult2B1b in other gluconeogenic tissues. Also, both HNF4α and Sult2B1b are involved in many other biological functions, further study may investigate the role this endogenous negative feedback regulation in other physiological or pathophysiological conditions.

My thesis study also demonstrated STS as a steroid sulfatase to regulated adipose tissue energy homeostasis. One interesting finding was that, STS in male mice decreased adipogenesis while in female mice increase adipogenesis, which was dependent on the androgen and estrogen signaling pathway respectively. Our previously study published that estrogen sulfotransferase EST could influence adipogenesis in adipocyte in a species-specific manner (114). Further study of STS may focus on investigating its adipogenic effect in primary adipocyte. Other interesting finding is that, STS also influence the thermogenic Ucp1 gene expression. Furthermore, energy expenditure of both male and female Tg mice were influenced by STS transgene. This pointed out another potential direction to study STS function in beige cell, which is a specific "adipocyte" in white adipose tissue, where Ucp1 is highly expressed regulating uncoupling ATP expenditure (115).

As the key enzyme to locally synthesize estrogen, STS has been found to play pathogenic role in hormone dependent cancers. It has been decades that researchers investigate STS inhibitors

to use as an anti-tumor drug (116). In this study, I demonstrated that STS in adipose tissue aggravated the HFD induced diabetic phenotypes in males and improve those in female mice. Therefore, inactivation of STS in males and activation in females could be potential therapeutic method to manage the metabolic disorders. Further study could continue to study the effect of STS substrate or the available inhibitors in energy homeostasis.

In a conclusion, I demonstrated Sult2B1b and STS though regulating the chemical and functional homeostasis of endogenous molecules, for example cholesterol and steroid hormones act significant role in energy homeostasis. Both of these enzymes could be potential therapeutic target for the management of metabolic syndromes.

BIBLIOGRAPHY

1. Evans, R. M. 1988. "The steroid and thyroid hormone receptor superfamily." Science 240(4854): 889-895.

2. Giguere, V. 1999. "Orphan nuclear receptors: from gene to function." Endocr Rev 20(5): 689- 725.

3. Carson-Jurica, M. A., W. T. Schrader and B. W. O'Malley 1990. "Steroid receptor family: structure and functions." Endocr Rev 11(2): 201-220.

4. Chawla, A., J. J. Repa, R. M. Evans, et al. 2001. "Nuclear receptors and lipid physiology: opening the X-files." Science 294(5548): 1866-1870.

5. Gonzalez FJ. 2008. Regulation of hepatocyte nuclear factor 4 alpha- mediated transcription. Drug Metab Pharmacokinet 23:2–7.

6. Shi X, Cheng Q, Xu L, Yan J, Jiang M, He J, Xu M, Stefanovic-Racic M, Sipula I, O' Doherty RM, Ren S, Xie W. 2014. Cholesterol sulfate and cholesterol sulfotransferase inhibit gluconeogenesis by targeting hepatocyte nuclear factor 4alpha. Mol Cell Biol 34:485–497.

7. Puigserver P, Rhee J, Donovan J, Walkey CJ, Yoon JC, Oriente F, Kitamura Y, Altomonte J, Dong H, Accili D, Spiegelman BM. 2003. Insulin-regulated hepatic gluconeogenesis through FOXO1-PGC-1alpha interaction. Nature 423:550 –555.

8. Rhee J, Inoue Y, Yoon JC, Puigserver P, Fan M, Gonzalez FJ, Spiegelman BM. 2003. Regulation of hepatic fasting response by PPARgamma coactivator-1alpha (PGC-1): requirement for hepatocyte nuclear factor 4alpha in gluconeogenesis. Proc Natl Acad Sci U S A 100:4012–4017.

9. Xie X, Liao H, Dang H, Pang W, Guan Y, Wang X, Shyy JY, Zhu Y, Sladek FM. 2009. Down-regulation of hepatic HNF4alpha gene expression during hyperinsulinemia via SREBPs. Mol Endocrinol 23:434 – 443.

10. Rizza RA. 2010. Pathogenesis of fasting and postprandial hyperglycemia in type 2 diabetes: implications for therapy. Diabetes 59:2697–2707.

11. Magnusson, I, Rothman DL, Katz LD, Shulman RG, Shulman GI. 1992. Increased rate of gluconeogenesis in type II diabetes mellitus. A 13C nuclear magnetic resonance study. J Clin Invest 90:1323–1327.

12. Yokoyama A, Katsura S, Ito R, Hashiba W, Sekine H, Fujiki R, Kato S. 2011. Multiple post-translational modifications in hepatocyte nuclear factor 4alpha. Biochem Biophys Res Commun 410:749–753.

13. Thakran S, Sharma P, Attia RR, Hori RT, Deng X, Elam MB, Park EA. 2013. Role of sirtuin 1 in the regulation of hepatic gene expression by thyroid hormone. J Biol Chem 288:807– 818.

14. Soutoglou E, Katrakili N, Talianidis I. 2000. Acetylation regulates transcription factor activity at multiple levels. Mol Cell 5:745–751.

15. Navarro, G., Allard, C., Xu, W., and Mauvais-Jarvis, F. 2015. The role of androgens in metabolism, obesity, and diabetes in males and females. Obesity (Silver Spring) 23:713-719

16. Oh JY, Barrett-Connor E, Wedick NM, Wingard DL, Rancho Bernardo S. 2002. Endogenous sex hormones and the development of type 2 diabetes in older men and women: the Rancho Bernardo study. Diabetes Care 25:55-60.

17. Carr MC. 2003. The emergence of the metabolic syndrome with menopause. J Clin Endocrinol Metab 88:2404-2411.

18. Margolis KL, Bonds DE, Rodabough RJ, Tinker L, Phillips LS, Allen C, Bassford T, Burke G, Torrens J, Howard BV, Women's Health Initiative I. 2004. Effect of oestrogen plus progestin on the incidence of diabetes in postmenopausal women: results from the Women's Health Initiative Hormone Trial. Diabetologia 47:1175-1187.

19. Smith EP, Boyd J, Frank GR, Takahashi H, Cohen RM, Specker B, Williams TC, Lubahn DB, Korach KS. 1994. Estrogen resistance caused by a mutation in the estrogen-receptor gene in a man. N Engl J Med 331:1056-1061.

20. Morishima A, Grumbach MM, Simpson ER, Fisher C, Qin K. 1995. Aromatase deficiency in male and female siblings caused by a novel mutation and the physiological role of estrogens. J Clin Endocrinol Metab 80:3689-3698.

21. Jones ME, Thorburn AW, Britt KL, Hewitt KN, Wreford NG, Proietto J, Oz OK, Leury BJ, Robertson KM, Yao S, Simpson ER. 2000. Aromatase-deficient (ArKO) mice have a phenotype of increased adiposity. Proc Natl Acad Sci U S A 97:12735-12740.

22. Smith, E. P., Boyd, J., Frank, G. R., Takahashi, H., Cohen, R. M., Specker, B., Williams, T. C., Lubahn, D. B., and Korach, K. S. 1994. Estrogen resistance caused by a mutation in the estrogen-receptor gene in a man. N Engl J Med 331:1056-1061

23. Morishima, A., Grumbach, M. M., Simpson, E. R., Fisher, C., and Qin, K. (1995) Aromatase deficiency in male and female siblings caused by a novel mutation and the physiological role of estrogens. J Clin Endocrinol Metab 80:3689-3698

24. Friday, K. E., Dong, C., and Fontenot, R. U. 2001. Conjugated equine estrogen improves glycemic control and blood lipoproteins in postmenopausal women with type 2 diabetes. J Clin Endocrinol Metab 86: 48-52

25. Billeci, A. M., Paciaroni, M., Caso, V., and Agnelli, G. 2008. Hormone replacement therapy and stroke. Curr Vasc Pharmacol 6:112-123

26. Ding EL, Song Y, Malik VS, Liu S. 2006. Sex differences of endogenous sex hormones and risk of type 2 diabetes: a systematic review and meta-analysis. JAMA 295:1288-1299.

27. Diamond MP, Grainger D, Diamond MC, Sherwin RS, Defronzo RA. 1998. Effects of methyltestosterone on insulin secretion and sensitivity in women. J Clin Endocrinol Metab 83:4420-4425.

28. Holmang A, Larsson BM, Brzezinska Z, Bjorntorp P. 1992. Effects of short-term testosterone exposure on insulin sensitivity of muscles in female rats. Am J Physiol 262: E851-855.

29. Holmang A, Svedberg J, Jennische E, Bjorntorp P. 1990. Effects of testosterone on muscle insulin sensitivity and morphology in female rats. Am J Physiol 259: E555-560.

30. Montes-Nieto R, Insenser M, Martinez-Garcia MA, Escobar-Morreale HF. 2013. A nontargeted proteomic study of the influence of androgen excess on human visceral and subcutaneous adipose tissue proteomes. J Clin Endocrinol Metab 98: E576-585.

31. Gambineri A, Fanelli F, Tomassoni F, Munarini A, Pagotto U, Andrew R, Walker BR, Pasquali R. 2014. Tissue-specific dysregulation of 11beta-hydroxysteroid dehydrogenase type 1 in overweight/obese women with polycystic ovary syndrome compared with weight-matched controls. Eur J Endocrinol 171:47-57.

32. Nohara K, Laque A, Allard C, Munzberg H, Mauvais-Jarvis F. 2014. Central mechanisms of adiposity in adult female mice with androgen excess. Obesity (Silver Spring) 22:1477-1484.

33. O'Meara NM, Blackman JD, Ehrmann DA, Barnes RB, Jaspan JB, Rosenfield RL, Polonsky KS. 1993. Defects in beta-cell function in functional ovarian hyperandrogenism. J Clin Endocrinol Metab 76:1241-1247.

34. Corona G, Monami M, Rastrelli G, Aversa A, Sforza A, Lenzi A, Forti G, Mannucci E, Maggi M. 2011. Type 2 diabetes mellitus and testosterone: a meta-analysis study. Int J Androl 34:528-540.

35. Grossmann M. 2011. Low testosterone in men with type 2 diabetes: significance and treatment. J Clin Endocrinol Metab 96:2341-2353.

36. Keating NL, O'Malley AJ, Smith MR. 2006. Diabetes and cardiovascular disease during androgen deprivation therapy for prostate cancer. J Clin Oncol 24:4448-4456.

37. Lin HY, Yu IC, Wang RS, Chen YT, Liu NC, Altuwaijri S, Hsu CL, Ma WL, Jokinen J, Sparks JD, Yeh S, Chang C. 2008. Increased hepatic steatosis and insulin resistance in mice lacking hepatic androgen receptor. Hepatology 47:1924-1935.

38. Livingstone DE, Barat P, Di Rollo EM, Rees GA, Weldin BA, Rog-Zielinska EA, MacFarlane DP, Walker BR, Andrew R. 2015. 5alpha-Reductase type 1 deficiency or inhibition predisposes to insulin resistance, hepatic steatosis, and liver fibrosis in rodents. Diabetes 64:447-458.

39. Volzke H, Aumann N, Krebs A, Nauck M, Steveling A, Lerch MM, Rosskopf D, Wallaschofski H. 2010. Hepatic steatosis is associated with low serum testosterone and high serum DHEAS levels in men. Int J Androl 33:45-53.

40. Palomar-Morales M, Morimoto S, Mendoza-Rodriguez CA, Cerbon MA. 2010. The protective effect of testosterone on streptozotocin-induced apoptosis in beta cells is sex specific. Pancreas 39:193-200.

41. Morimoto S, Cerbon MA, Alvarez-Alvarez A, Romero-Navarro G, Diaz-Sanchez V. 2001. Insulin gene expression pattern in rat pancreas during the estrous cycle. Life Sci 68:2979-2985.

42. Haren MT, Siddiqui AM, Armbrecht HJ, Kevorkian RT, Kim MJ, Haas MJ, Mazza A, Kumar VB, Green M, Banks WA, Morley JE. 2011. Testosterone modulates gene expression pathways regulating nutrient accumulation, glucose metabolism and protein turnover in mouse skeletal muscle. Int J Androl 34:55-68.

43. Mootha VK, Lindgren CM, Eriksson KF, Subramanian A, Sihag S, Lehar J, Puigserver P, Carlsson E, Ridderstrale M, Laurila E, Houstis N, Daly MJ, Patterson N, Mesirov JP, Golub TR, Tamayo P, Spiegelman B, Lander ES, Hirschhorn JN, Altshuler D, Groop LC. 2003. PGC-1alpha-responsive genes involved in oxidative phosphorylation are coordinately downregulated in human diabetes. Nat Genet 34:267-273.

44. Khaw KT, Barrett-Connor E. 1992. Lower endogenous androgens predict central adiposity in men. Ann Epidemiol 2:675-682.

45. Pitteloud N, Mootha VK, Dwyer AA, Hardin M, Lee H, Eriksson KF, Tripathy D, Yialamas M, Groop L, Elahi D, Hayes FJ. 2005. Relationship between testosterone levels, insulin sensitivity, and mitochondrial function in men. Diabetes Care 28:1636-1642.

46. Gentile MA, Nantermet PV, Vogel RL, Phillips R, Holder D, Hodor P, Cheng C, Dai H, Freedman LP, Ray WJ. 2010. Androgen-mediated improvement of body composition and muscle function involves a novel early transcriptional program including IGF1, mechano growth factor, and induction of {beta}-catenin. J Mol Endocrinol 44:55-73.

47. Fernando SM, Rao P, Niel L, Chatterjee D, Stagljar M, Monks DA. 2010. Myocyte androgen receptors increase metabolic rate and improve body composition by reducing fat mass. Endocrinology 151:3125-3132.

48. Yu IC, Lin HY, Liu NC, Wang RS, Sparks JD, Yeh S, Chang C. 2008. Hyperleptinemia without obesity in male mice lacking androgen receptor in adipose tissue. Endocrinology 149:2361-2368.

49. Strott, C.A. 2002. Sulfonation and molecular action. Endocr. Rev. 23:703-732.

50. Gong, H.B., Guo, P., Zhai, Y., Zhou, J., Uppal, H., Jarzynka, M.J., Song, W.C., Cheng, S.Y., and Xie, W. 2007. Estrogen deprivation and inhibition of breast cancer growth in vivo through activation of the orphan nuclear receptor liver X receptor. Mol. Endocrinol. 21:1781-1790.

51. Lee, J.H., Gong, H., Khadem, S., Lu, Y., Gao, X., Li, S., Zhang, J., and Xie, W. 2008. Androgen deprivation by activating the liver X receptor. Endocrinology 149:3778-3788.

52. Shimizu, C., Fuda, H., Yanai, H., and Strott, C.A. 2003. Conservation of the hydroxysteroid sulfotransferase SULT2B1 gene structure in the mouse: Pre- and postnatal expression, kinetic analysis of isoforms, and comparison with prototypical SULT2A1. Endocrinology. 144:1186-1193.

53. Javitt, N.B., Lee, Y.C., Shimizu, C., Fuda, H., and Strott, C.A. 2001. Cholesterol and hydroxycholesterol sulfotransferases: identification, distinction from dehydroepiandrosterone sulfotransferase, and differential tissue expression. Endocrinology. 142:2978-2984.

54. Shimizu, C., Fuda, H., Yanai, H., and Strott, C. A. 2003. Endocrinology 144,1186–1193 Shimizu, C., Fuda, H., Yanai, H., and Strott, C.A. 2003. Conservation of the hydroxysteroid sulfotransferase SULT2B1 gene structure in the mouse: Pre- and postnatal expression, kinetic analysis of isoforms, and comparison with prototypical SULT2A1. Endocrinology. 144:1186-1193.

55. Strott, C.A., and Higashi, Y. 2003. Cholesterol sulfate in human physiology: what's it all about? J Lipid Res 44:1268-1278.

56. Dong, B., Saha, P.K., Huang, W.D., Chen, W.L., Abu-Elheiga, L.A., Wakil, S.J., Stevens, R.D., Ilkayeva, O., Newgard, C.B., Chan, L., Moore, D.D. 2009. Activation of nuclear receptor CAR ameliorates diabetes and fatty liver disease. P. Natl. Acad. Sci. USA 106:18831-18836.

57. Tamasawa, N., Tamasawa, A., and Takebe, K. 1993. Higher levels of plasma cholesterol sulfate in patients with liver cirrhosis and hypercholesterolemia. Lipids 28:833-836.

58. Veares, M.P., Evershed, R.P., Prescott, M.C., and Goad, L.J. 1990. Quantitative-determination of cholesterol sulfate in plasma by stable isotope-dilution fast-atom-bombardment mass-spectrometry. Environ. Mass 19:583-588.

59. Drayer, N.M., and Lieberman, S. 1967. Isolation of cholesterol sulfate from human aortas and adrenal tumors. J. Clin. Endocrinol. Metab. 27:136-139.

60. Kallen, J., Schlaeppi, J.M., Bitsch, F., Delhon, I., and Fournier, B. 2004. Crystal structure of the human RORalpha Ligand binding domain in complex with cholesterol sulfate at 2.2 A. J. Biol. Chem. 279:14033-14038.

61. Seneff, S., Davidson, R., and Mascitelli, L. 2012. Might cholesterol sulfate deficiency contribute to the development of autistic spectrum disorder? Med. Hypotheses. 78:213-217.

62. Yamamoto, K., Miyazaki, K., and Higashi, S. 2010. Cholesterol sulfate alters substrate preference of matrix metalloproteinase-7 and promotes degradations of pericellular laminin-332 and fibronectin. J. Biol. Chem. 285:28862-28873.

63. Ferrante, P., Messali, S. 2002. Molecular and biochemical characterisation of a novel sulphatase gene: Arylsulfatase G (ARSG). European Journal of Human Genetics, 10(12), 813–818.

64. Leowattana, W. 2004. DHEAS as a new diagnostic tool. Clinica Chimica Acta, 341(1–2), 1–15.

65. Pasqualini, J. R. 2004. The selective estrogen enzyme modulators in breast cancer: A review. Biochimica et Biophysica Acta, 1654(2), 123–143.

66. Mueller, J. W., Gilligan, L. C., et al. 2015. The regulation of steroid action by sulfation and desulfation. Endocrine Reviews, 36(5), 526–563. 36.

67. Egyed J, Oakey RE. 1985. Hydrolysis of deoxycorticosterone-21-yl sulphate and dehydroepiandrosterone sulphate by microsomal preparations of human placentae: evidence for a common enzyme. J Endocrinol 106:295-301.

68. Dibbelt L, Kuss E. 1983. Human placental steroid-sulfatase. Kinetics of the in-vitro hydrolysis of dehydroepiandrosterone 3-sulfate and of 16 alpha-hydroxydehydroepiandrosterone 3-sulfate. Hoppe Seylers Z Physiol Chem 364:187-191.

69. Kester MH, Kaptein E, Van Dijk CH, Roest TJ, Tibboel D, Coughtrie MW, Visser TJ. 2002. Characterization of iodothyronine sulfatase activities in human and rat liver and placenta. Endocrinology 143:814-819.

70. Webster, D., France, J. T., et al. 1978. X-linked ichthyosis due to steroid-sulphatase deficiency. Lancet, 1(8055), 70–72.

71. Pasquali, R., Vicennati, V. 2008. Sex-dependent role of glucocorticoids and androgens in the pathophysiology of human obesity. International Journal of Obesity, 32(12), 1764–1779.

72. Jiang M, He J, Kucera H, Gaikwad NW, Zhang B, Xu M, et al. 2014. Hepatic overexpression of steroid sulfatase ameliorates mouse models of obesity and type 2 diabetes through sex-specific mechanisms. J Biol Chem. 289(12):8086-97.

73. Paatela, H., Wang, F. 2016. Steroid sulfatase activity in subcutaneous and visceral adipose tissue: A comparison between pre- and postmenopausal women. European Journal of Endocrinology, 174(2), 167–175.

74. Yuan X, Ta TC, Lin M, Evans JR, Dong Y, Bolotin E, Sherman MA, Forman BM, Sladek FM. 2009. Identification of an endogenous ligand bound to a native orphan nuclear receptor. PLoS One 4: e5609.

75. Kiselyuk A, Lee SH, Farber-Katz S, Zhang M, Athavankar S, Cohen T, Pinkerton AB, Ye M, Bushway P, Richardson AD, Hostetler HA, Rodriguez- Lee M, Huang L, Spangler B, Smith L, Higginbotham J, Cashman J, Freeze H, Itkin-Ansari P, Dawson MI, Schroeder F, Cang Y, Mercola M, Levine F. 2012. HNF4alpha antagonists discovered by a high-throughput screen for modulators of the human insulin promoter. Chem Biol 19:806 – 818.

76. Fang B, Mane-Padros D, Bolotin E, Jiang T, Sladek FM. 2012. Identification of a binding motif specific to HNF4 by comparative analysis of multiple nuclear receptors. Nucleic Acids Res 40:5343–5356.

77. Sone H, Shimano H, Sakakura Y, Inoue N, Amemiya-Kudo M, Yahagi N, Osawa M, Suzuki H, Yokoo T, Takahashi A, Iida K, Toyoshima H, Iwama A, Yamada N. 2002. Acetyl-coenzyme A synthetase is a lipogenic enzyme controlled by SREBP-1 and energy status. Am J Physiol Endocrinol Metab 282: E222–E230.

78. Cho YS, Chen CH, Hu C, Long J, Ong RT, Sim X, Takeuchi F, Wu Y, Go MJ, Yamauchi T, Chang YC, Kwak SH, Ma RC, Yamamoto K, Adair LS, Aung T, Cai Q, Chang LC, Chen YT, Gao Y, Hu FB, Kim HL, Kim S, Kim YJ, Lee JJ, Lee NR, Li Y, Liu JJ, Lu W, Nakamura J, Nakashima E, Ng DP, Tay WT, Tsai FJ, Wong TY, Yokota M, Zheng W, Zhang R, Wang C, So WY, Ohnaka K, Ikegami H, Hara K, Cho YM, Cho NH, Chang TJ, Bao Y, Hedman AK, Morris AP, McCarthy MI, DIAGRAM Consortium; MuTHER Consortium, Takayan- agi R, Park KS, Jia W, Chuang LM, Chan JC, Maeda S, Kadowaki T, Lee JY, Wu JY, Teo YY, Tai ES, Shu XO, Mohlke KL, Kato N, Han BG, Seielstad M. 2011. Meta-analysis of genome-wide association studies identifies eight new loci for type 2 diabetes in east Asians. Nat Genet 44:67–72.

79. Johansson S, Raeder H, Eide SA, Midthjell K, Hveem K, Sovik O, Molven A, Njolstad PR. 2007. Studies in 3,523 Norwegians and meta- analysis in 11,571 subjects indicate that variants in the hepatocyte nuclear factor 4 alpha (HNF4A) P2 region are associated with type 2 diabetes in Scandinavians. Diabetes 56:3112–3117.

80. Yang X, Xu Y, Guo F, Ning Y, Zhi X, Yin L, Li X. 2013. Hydroxysteroid sulfotransferase SULT2B1b promotes hepatocellular carcinoma cells proliferation in vitro and in vivo. PLoS One 8: e60853.

81. Vickman RE, Crist SA, Kerian K, Eberlin L, Cooks RG, Burcham GN, Buhman KK, Hu CD, Mesecar AD, Cheng L, Ratliff TL. 2016. Cholesterol sulfonation enzyme, SULT2B1b, modulates AR and cell growth properties in prostate cancer. Mol Cancer Res 14:776–786.

82. Wang F, Beck-Garcia K, Zorzin C, Schamel WW, Davis MM. 2016. Inhibition of T cell receptor signaling by cholesterol sulfate, a naturally occurring derivative of membrane cholesterol. Nat Immunol 17:844 – 850.

83. Hwang-Verslues WW, Sladek FM. 2010. HNF4alpha–role in drug metabolism and potential drug target? Curr Opin Pharmacol 10:698–705.

84. Hundal RS, Krssak M, Dufour S, Laurent D, Lebon V, Chandramouli V, Inzucchi SE, Schumann WC, Petersen KF, Landau BR, Shulman GI. 2000. Mechanism by which metformin reduces glucose production in type 2 diabetes. Diabetes 49:2063–2069.

85. Vernon RG & Clegg RA. 1985. The metabolism of white adipose tissue in vivo and in vitro. New perspectives in adipose tissue: structure, function and development. London: Butterworths, pp. 65–86.

86. Trayhurn P. 2013. Hypoxia and adipose tissue function and dysfunction in obesity. Physiological Reviews 93: 1–21.

87. Siiteri PK. 1987. Adipose tissue as a source of hormones. American Journal of Clinical Nutrition 45: 277–282.

88. Van Gaal LF, Mertens IL & De Block CE. 2006. Mechanisms linking obesity with cardiovascular disease. Nature 444: 875–880.

89. Blüher M. 2009. Adipose tissue dysfunction in obesity. Experimental and Clinical Endocrinology & Diabetes 117: 241–250.

90. Bays HE. 2011. Adiposopathy is "sick fat" a cardiovascular disease? Journal of the American College of Cardiology 57: 2461–2473.

91. Cancello R, Henegar C, Viguerie N. 2005. Reduction of macrophage infiltration and chemoattractant gene expression changes in white adipose tissue of morbidly obese subjects after surgery-induced weight loss. Diabetes 54: 2277– 2286.

92. Harman-Boehm I, Blüher M, Redel H. 2007. Macrophage infiltration into omental versus subcutaneous fat across different populations: effect of regional adiposity and the comorbidities of obesity. Journal of Clinical Endocrinology & Metabolism 92: 2240–2247.

93. He, J., Gao, J., Xu, M., Ren, S., Stefanovic-Racic, M., O'Doherty, R. M., and Xie, W. 2013. PXR ablation alleviates diet-induced and genetic obesity and insulin resistance in mice. Diabetes 62: 1876-1887.

94. Xie, W., Barwick, J. L., Downes, M., Blumberg, B., Simon, C. M., Nelson, M. C., Neuschwander-Tetri, B. A., Brunt, E. M., Guzelian, P. S., and Evans, R. M. 2000. Humanized xenobiotic response in mice expressing nuclear receptor SXR. Nature 406: 435-439.

95. Gao, J., He, J., Zhai, Y., Wada, T., and Xie, W. 2009. The constitutive androstane receptor is an anti-obesity nuclear receptor that improves insulin sensitivity. J Biol Chem 284:25984-25992.

96. Gaikwad, N. W. 2013. Ultra-performance liquid chromatography-tandem mass spectrometry method for profiling of steroid metabolome in human tissue. Anal Chem 85, 4951-4960

97. Keating NL, O'Malley AJ, Smith MR. 2006. Diabetes and cardiovascular disease during androgen deprivation therapy for prostate cancer. J Clin Oncol 24:4448-4456.

98. Bjorndal B, Burri L, Staalesen V, Skorve J, Berge RK. 2011. Different adipose depots: their role in the development of metabolic syndrome and mitochondrial response to hypolipidemic agents. J Obes 2011:490650.

99. Bickerton AST, Roberts R, Fielding BA, Hodson L, Blaak EE, et al. 2007. Preferential uptake of dietary fatty acids in adipose tissue and muscle in the postprandial period. Diabetes. 56:168–176.

100. Anghel, S.I. and W. Wahli. 2007. Fat poetry: a kingdom for PPAR gamma. Cell Res 17: 486-511.

101. Spiegelman, B.M. 2007. PPAR-gamma: adipogenic regulator and thiazolidinedione receptor. Diabetes. 47:507-514.

102. Font de Mora, J., A. Porras, N. Ahn, and E. 1997. Santos. Mitogen-activated protein kinase activation is not necessary for, but antagonizes, 3T3-L1 adipocytic differentiation. Mol Cell Biol. 17, 6068-75.

103. Sale, E. M., P. G. Atkinson, and G. J. Sale. Requirement of MAP kinase for differentiation of fibroblasts to adipocytes, for insulin activation of p90 S6 kinase and for insulin or serum stimulation of DNA synthesis. 1995. EMBO J. 14, 674-84. Mothe-Satney I, Filloux C, Amghar H, Pons C, Bourlier V, Galitzky J, Grimaldi PA, Feral CC, Bouloumie A, Van Obberghen E, Neels JG. 2012. Adipocytes secrete leukotrienes: contribution to obesity-associated inflammation and insulin resistance in mice. Diabetes. 61:2311-2319.

104. Zhang Y, Calvo E, Martel C, Luu-The V, Labrie F, Tchernof A. 2008. Response of the adipose tissue transcriptome to dihydrotestosterone in mice. Physiol Genomics. 35:254-261

105. Jiang M, Klein M, Zanger UM, Mohammad MK, Cave MC, Gaikwad NW, Dias NJ, Selcer KW, Guo Y, He J et al. 2016. Inflammatory regulation of steroid sulfatase: A novel mechanism to control estrogen homeostasis and inflammation in chronic liver disease. J Hepatol. 64(1), 44-52.

106. Moverare-Skrtic S, Venken K, Andersson N, Lindberg MK, Svensson J, Swanson C, et al. 2006. Dihydrotestosterone treatment results in obesity and altered lipid metabolism in orchidectomized mice. Obesity (Silver Spring).14:662-672.

107. Finkelstein JS, Lee H, Burnett-Bowie SA, Pallais JC, Yu EW, Borges LF, et al. 2013. Gonadal steroids and body composition, strength, and sexual function in men. New England J Med.369:1011-1022.

108. Lanfranco F, Zitzmann M, Simoni M, Nieschlag E. 2004. Serum adiponectin levels in hypogonadal males: influence of testosterone replacement therapy. Clinical Endocrinol. 60:500-507.

109. Nishizawa H, Shimomura I, Kishida K, Maeda N, Kuriyama H, Nagaretani H, et al. 2002. Androgens decrease plasma adiponectin, an insulin-sensitizing adipocyte-derived protein. Diabetes. 51:2734-2741.

110. Berg AH, Combs TP, Du X, Brownlee M, Scherer PE. The adipocyte-secreted protein Acrp30 enhances hepatic insulin action. Nat Med. 7:947-953.

111. Kubota N, Hara K, Mori Y, Ide T, Murakami K, Tsuboyama-Kasaoka N, Ezaki O, Akanuma Y, Gavrilova O, Vinson C, Reitman ML, Kagechika H, Shudo K, Yoda M, Nakano Y, Tobe K, Nagai R, Kimura S, Tomita M, Froguel P, Kadowaki T. 2001. The fat-derived hormone adiponectin reverses insulin resistance associated with both lipoatrophy and obesity. Nat Med. 7:941-946.

112. Fu M, Sun T, Bookout AL, Downes M, Yu RT, Evans RM, Mangelsdorf DJ. 2005. A Nuclear Receptor Atlas: 3T3-L1 adipogenesis. Mol Endocrinol. 19:2437-2450.

113. Gao J, He J, Shi X, Stefanovic-Racic M, Xu M, O'Doherty RM, Garcia-Ocana A, Xie W. 2012. Sex-specific effect of estrogen sulfotransferase on mouse models of type 2 diabetes. Diabetes. 61(6):1543-1551

114. Garbacz, W.G., Jiang, M., Xu, M., Yamauchi, J., Dong, H.H., and Xie, W. 2017. Sex- and Tissue-Specific Role of Estrogen Sulfotransferase in Energy Homeostasis and Insulin Sensitivity. Endocrinology.158:4093-4104

115. Svensson, K.J. et al. 2016. A Secreted Slit2 Fragment Regulates Adipose Tissue Thermogenesis and Metabolic Function. Cell Metab 23:454-466

116. Sadozai, H. 2013. Steroid sulfatase inhibitors: promising new therapy for breast cancer. J Pak Med Assoc 63:509-51.